# Role of mPFC DUSP1 in regulating the sensitivity to cocaine in adolescent cocaine-exposed mice of adulthood

Xiaoyan Wei[1,2], Zhen Cheng[1,2], Wenwen Chen[1], Hao Guo[1], Zhaoyu Liu[1], Tao Hu[1], Yuanyuan Zhang[1], Qinglong Cai[1], Feifei Ge[1], Yu Fan[1,*], Jiasong Chang[1,*], Xiaowei Guan[1,*]

[1]Department of Human Anatomy and Histoembryology, Nanjing University of Chinese Medicine, Nanjing, China

[2]These authors are equally contribute to this work

**Running title**: Adolescent cocaine and mPFC DUSP1

*Correspondence to: Prof. Xiaowei Guan (guanxw918@njucm.edu.cn), Dr. Yu Fan (yfan@njucm.edu.cn) and Dr. Jiasong Chang (331880557@qq.com)

Phone number: +86-15295560773

**Abstract**

Cocaine abuse during adolescence increases the risk for developing drug addiction in later life, but the underlying molecular mechanism remains unclear. Here, adolescent cocaine-exposed (ACE) male mice models were established by giving once-daily intraperitoneal injections of 15 mg/kg cocaine to mice during adolescence (P28-P42). We found that ACE mice exhibited a higher sensitivity to subthreshold dose of cocaine (1 mg/kg) in adulthood, accompanied with triggered activities and dendritic spine density of pyramidal neuron, increased *Dusp1* gene, as well as reduced protein levels and activity of dual specificity phosphatase 1 (DUSP1) in mPFC. Specific overexpression of DUSP1 on mPFC glutamatergic neurons efficiently blocked cocaine-preferred behaviors and reduced mPFC activity, while knockdown of DUSP1 maintained cocaine-preferred behaviors and increased mPFC activity in ACE mice. MAPK-related signals, especially ERK1/2, might underlie the mediating effects of DUSP1. Collectively, these findings suggested that targeting mPFC DUSP1 may represent a promising therapeutic strategy for the treatment and attenuation of addiction susceptibility, particularly in addicts with a history of adolescent drugs exposure.

**Keywords:** adolescent cocaine exposure, adulthood, sensitivity to drugs, mPFC, DUSP1

## Significance statement

Cocaine-exposed experience during adolescence enhances the sensitivity of mice to drugs and triggers more activity of medial prefrontal cortex (mPFC) in adulthood, which is rescued by specific overexpression of dual specificity phosphatase 1 (DUSP1) on glutamatergic neurons of mPFC. MAPK-related signals, especially ERK1/2, might underlie the regulatory effects of DUSP1.

## Introduction

Adolescents are more susceptible to toxicity of drugs such as cocaine than adults (1-3). Adolescent cocaine use increases the risk for developing drug addiction in later life, depending on both social environment and biological vulnerability to drugs (4, 5), but the underlying biological molecules remains unclear.

As a critical period of neurodevelopment, adolescent brain undergoes essential orchestrating process by neuronal reorganization, neurogenesis and pruning (6). In adolescence, medial prefrontal cortex (mPFC) is still in a state of rapid development (7-9). The mPFC has been well-studied in the susceptibility to drugs addiction (10, 11). A single cocaine treatment to adolescent rather than adult animals alters density of dendritic spines and glutamate receptor function in mPFC (12, 13), indicating susceptibility of mPFC to toxic effects of drugs in adolescents (14, 15). Previously, we found that adolescent cocaine exposure (ACE) enhanced the GABAergic transmission on pyramidal neurons of mPFC (16) and produced a prolonged modification on mPFC synapses in adult rodents (17). Anatomically, mPFC is divided into subregions of cingulate cortex (Cg1), prelimbic cortex (PrL) and infralimbic cortex (IL), each sending distinct glutamatergic excitatory projections to limbic structures (18-21). Further, the rodent mPFC consists of distinct cytoarchitectonic layers (Layers 1–6), and glutamatergic pyramidal neurons occupy about 85% of neurons in Layers of 2/3 and 5/6 (22, 23). Glutamatergic output from the mPFC is critically implicated in encoding cocaine-induced behavioral sensitization (20, 24, 25). However, the molecular mechanisms of mPFC underlying the ACE-promoted susceptibility of adult mice to drugs remains unclear.

The dual specificity protein kinase-phosphatase-1 (DUSP1), also known as mitogen-activated protein kinase-phosphatase-1 (MKP-1), is a negative regulatory factor on the activation of mitogen activated protein kinases (MAPKs) (26). By regulating dephosphorylation of MAPKs such as ERK1/2, p38 and the c-Jun N-terminal kinases (JNKs), DUSP1 has been proved to achieve neuroprotection in hearing loss (27), Huntington's disease (28), cerebral ischemia reperfusion injury (29) and neuropathic pain (30) through anti-inflammatory, antioxidant, mitochondrial repair and supporting axon survival functions. In addition, *Dusp1* gene are known to be activity-dependent responded to stimuli signals in the brain, thus often acts as an immediate early gene (IEGs) like *c-fos*. For example, psilocybin strongly upregulates *Dusp1* levels in PFC (31), while synthetic cathinone (substitutes for illicit psychostimulants including cocaine) produces increased mRNA levels of *Dusp1* in striatum (32), which may underlie addictive potential of drugs of abuse.

In the present study, ACE mice model was established by exposing adolescent male mice to cocaine from postnatal day 28 (P28) to P42 (33). When mice growing up to adult age, ACE mice were subjected to CPP behaviors with subthreshold doses of cocaine to evaluate their susceptibility to drugs, and the role of mPFC DUSP1 were explored in the enhanced sensitivity of ACE mice to cocaine in their adulthood.

## Results

### Subthreshold doses of cocaine elicits cocaine-preferred behaviors and triggers mPFC activity in ACE mice of adulthood

To examine the sensitivity of adult mice to cocaine, mice were subjected to subthreshold doses of cocaine-induced CPP training and tests (Figure 1A). As shown in Figure 1B-D, subthreshold doses of cocaine failed to induce CPP behaviors in adolescent saline

exposed (ASE-C) mice (n = 28, $t$ = 0.8324, $p$ = 0.6503), but produced cocaine-preferred behaviors in adolescent cocaine exposed (ACE-C) mice (n = 31, $t$ = 6.761, $p$ < 0.0001, Figure 1B, 1D). The ΔCPP score was higher in ACE-C mice than that in ASE-C mice (n = 59, $t$ = 4.054, $p$ = 0.0002, Figure 1C, 1D).

To mapping the brain activity in respond to subthreshold-dosed administration of cocaine in adult mice, c-Fos, NeuN, CaMKII, GAD67, PV and SOM were used as markers to evaluate neuronal activation and to label neuron, glutamatergic neuron, GABAergic neuron, PV-positive GABAergic neuron and SOM-positive GABAergic neuron, respectively. Compared with ASE-C mice of adulthood, the c-Fos-stained levels of neurons is much higher in mPFC (n = 12, $t$ = 2.89, $p$ = 0.0161) and its subregions of cingulate cortex (Cg1, n = 12, $t$ = 2.912, $p$ = 0.0155) and prelimbic cortex (PrL, n = 12, $t$ = 2.311, $p$ = 0.0435), but similar in infralimbic cortex (IL, n = 12, $t$ = 0.8092, $p$ = 0.4372, Figure 1E), orbitofrontal cortex (OFC, n = 12, $t$ = 2.055, $p$ = 0.0670), nucleus accumbens core (NAc core, n = 12, $t$ = 0.3219, $p$ = 0.7542), nucleus accumbens shell (NAc shell, n = 12, $t$ = 1.632, $p$ = 0.1337), bed nucleus of the stria terminalis (BNST, n = 12, $t$ = 1.172, $p$ = 0.2685), triangular septal nucleus (TS, n = 12, $t$ = 1.768, $p$ = 0.1074), basolateral amygdala (BLA, n = 12, $t$ = 1.304, $p$ = 0.2215), central nucleus of the amygdala (CeA, n = 12, $t$ = 0.2851, $p$ = 0.7814), medial habenula (mHb, n = 12, $t$ = 0.2165, $p$ = 0.8329), lateral habenular (LHb, n = 12, $t$ = 1.151, $p$ = 0.2764), dorsal hippocampal CA1 (dCA1, n = 12, $t$ = 0.09203, $p$ = 0.9285), dorsal hippocampal CA3 (dCA3, n = 12, $t$ = 0.6802, $p$ = 0.5118), dorsal dentate gyrus (dDG, n = 12, $t$ = 0.5304, $p$ = 0.6074), ventral hippocampal CA1 (vCA1, n = 10, $t$ = 0.1572, $p$ = 0.8790) and ventral tegmental area (VTA, n = 12, $t$ = 0.2915, $p$ = 0.7767, Figure S1A) in ACE-C mice of adulthood.

On P74 before cocaine CPP training, the c-Fos protein levels (n = 6, $t$ = 5.899, $p$ = 0.0041, Figure S2A) of mPFC is significantly higher in ACE than that in ASE mice of adulthood. And on P78 following cocaine CPP test, the c-Fos protein levels (n = 6, $t$ = 4.748, $p$ = 0.0090, Figure S2A) and dendritic spine density (n = 6, $t$ = 5.575, $p$ = 0.0051, Figure 1F) of mPFC is significantly higher in ACE-C than that in ASE-C mice of adulthood. In parallel, the levels of c-Fos-stained neurons in layer2/3 of Cg1 (n = 12, $t$ = 3.366, $p$ = 0.0072) and in layer5 of Cg1 (n = 12, $t$ = 3.621, $p$ = 0.0047), PrL (n = 12, $t$ = 2.572, $p$ = 0.0278) were higher, while in layer2/3 of PrL (n = 12, $t$ = 1.526, $p$ = 0.1579), IL (n = 12, $t$ = 0.2772, $p$ = 0.7873) and in layer 5 of IL (n = 12, $t$ = 1.222, $p$ = 0.2498) were similar in ACE-C mice than that in ASE-C mice of their adulthood (Figure S2B). In ACE-C mice, the c-Fos staining in total mPFC (n = 6, r = 0.9048, $p$ = 0.0132), Cg1 (n = 6, r = 0.9206, $p$ = 0.0092) and PrL (n = 6, r = 0.8646, $p$ = 0.0262), but not in IL (n = 6, r = 0.4181, $p$ = 0.4094) showed significant and positive correlation with the corresponding ΔCPP score (Figure S2C). Further, the c-Fos-stained CaMKII-positive glutamatergic neurons (n = 12, $t$ = 3.656, $p$ = 0.0044), but not GAD67-psositive GABAergic neurons (n = 12, $t$ = 1.180, $p$ = 0.2652) and its subtypes of PV-positive (n = 12, $t$ = 0.5668, $p$ = 0.5833) and SOM-positive neurons (n = 12, $t$ = 0.6119, $p$ = 0.5543), were much more in numbers at mPFC of ACE-C mice than that in ASE-C mice of adulthood (Figure S2D).

To record real-time calcium signals of mPFC CaMKII-positive glutamatergic neurons ($mPFC^{CaMKII}$) *in vivo*, *rAAV2/9-CaMKII-GCaMp6m-WPRE-PA* virus were injected into mPFC of adult mice, specially limiting to subregions of Cg1 and PrL (Figure 1G). Similarly to naïve mice, the subthreshold doses of cocaine induced cocaine-preferred behaviors in ACE-C-AAV mice (n = 8, $t$ = 5.699, $p$ = 0.0001) but not in ASE-C-AAV mice (n = 7, $t$ = 2.196, $p$ = 0.0914, Figure 1H), accompanied by a higher

ΔCPP score in ACE-C-AAV mice than that in ASE-C-AAV mice (n = 15, $t$ = 2.289, $p$ = 0.0395, Figure 1I, J). At first 4 sec-duration when mice entering into the cocaine-paired chamber, the calcium signals of mPFC$^{CaMKII}$ neurons were increased when compared to "zero" point of baseline in all GCaMp6m-transfected mice, and the calcium signals in mPFC$^{CaMKII}$ neurons were significantly higher, as indicated by AUC value (n = 6, $t$ = 3.839, $p$ = 0.0185) in ACE-C-AAV mice than that in ASE-C-AAV mice (Figure 1K-M).

**Subthreshold doses of cocaine increases *Dusp1* gene but decreases DUPS1 protein and activity in mPFC of adult ACE mice**

To screen potential molecules that contribute to the higher mPFC activity and cocaine-preferred behaviors, the RNA sequencing was performed in mPFC on P78 following CPP test. As shown in Figure S3A, following subthreshold-dosed administration of cocaine, 180 genes were upregulated and 248 genes were downregulated in mPFC of ACE-C mice, when compared to ASE-C mice. Among of them, *Dusp1* gene is one of the most significantly upregulated genes. By qPCR verification, the mRNA level of mPFC *Dusp1* were much higher in response to subthreshold doses of cocaine in ACE (ACE-C) than in ASE (ASE-C) mice (n = 11, $t$ = 4.100, $p$ = 0.0027, Figure 2A). According to Protein-Protein Interaction (PPI) network analysis of upregulated genes (Figure S3B) and heatmaps of top 40 upregulated genes (Figure S3C), *Dusp1* was a key and hub interactor gene that associated with other upregulated genes including *c-Fos*. Further, MAPK-related signals were both in the top 30 enriched GO (Figure S3D) and the top enriched 20 KEGG pathway (Figure S3E) of upregulated genes in mPFC of ACE-C mice, indicating that DSUP1 and related MAPK signals should be a critical molecule in mPFC that might be implicated in the increased susceptibility of ACE mice to cocaine.

The baseline level and responsive level to cocaine of DUSP1 protein and activity in mPFC of adult mice were examined on P74 and P78, respectively. As shown in Figure S4A-B, there is similar baseline level of mPFC DUSP1 (n = 6, $t$ = 1.905, $p$ = 0.1295, Figure S4A) and activity (n = 6, $t$ = 0.1855, $p$ = 0.8618, Figure S4B) between ACE and ASE mice on P74. However, on P78 after CPP test, subthreshold doses of cocaine produced an attenuation of DUSP1 protein level (n = 6, $t$ = 4.929, $p$ = 0.0079, Figure 2B), activity (n = 12, $t$ = 3.240, $p$ = 0.0089, Figure 2C) and staining value on CaMKII-positive neurons (n = 6, $t$ = 3.358, $p$ = 0.0283, Figure 2D) in mPFC of ACE-C, when compared to ASE-C mice.

The protein levels of MAPK-related signal molecules, including ERK1/2, CREB and BDNF, were examined in mPFC of adult mice on P78. As shown in Figure 2E, the levels of ratio of p-ERK to ERK (n = 6, $t$ = 3.338, $p$ = 0.0289), p-ERK (n = 6, $t$ = 3.143, $p$ = 0.0348), ratio of p-CREB/CREB (n = 6, $t$ = 6.340, $p$ = 0.0032), p-CREB (n = 6, $t$ = 4.615, $p$ = 0.0099), and BDNF (n = 6, $t$ = 2.781, $p$ = 0.0498) were significantly higher in ACE-C than that in ASE-C mice, while levels of ERK (n = 6, $t$ = 1.030, $p$ = 0.3611) and CREB (n = 6, $t$ = 0.04476, $p$ = 0.9664) were not different between groups.

**Overexpression of DUSP1 blocks cocaine-induced CPP behaviors and attenuates mPFC activity in ACE mice of adulthood**

To explore the role of mPFC DUSP1 in cocaine-preferred behaviors in ACE mice, *AAV9-CaMKII-DUSP1-RNAOE-EGFP* (OE virus) and *AAV9-CaMKII-EGFP* (Ctrl virus) were bilaterally infused into mPFC, especially to Cg1 and PrL, to overexpress DUSP1 in pyramidal neurons of mPFC (Figure 3A-B). As shown in Figure 3C, about 80% CaMKII-positive pyramidal neurons within injection sites were transfected with virus. Compared to ACE-C mice with Ctrl virus (ACE-$C_{Ctrl}$ mice), mPFC levels of mRNA (n = 6, $t$ = 4.413, $p$ = 0.0116, Figure 3D), protein (n = 6, $t$ = 4.071, $p$ = 0.0152,

Figure 3E) and activity (n = 12, $t$ = 3.336, $p$ = 0.0075, Figure 3F) of DUSP1 were all much higher in ACE-C mice with OE virus (ACE-$C_{OE}$ mice) after cocaine CPP test. Further, subthreshold-dosed administration of cocaine produced cocaine-preferred behaviors in ACE-$C_{Ctrl}$ mice (n = 14, $t$ = 2.521, $p$ = 0.0355) but not in ACE-$C_{OE}$ mice (n = 15, $t$ = 0.9970, $p$ = 0.5479), accompanied by a lower ΔCPP score in ACE-$C_{OE}$ mice (n = 29, $t$ = 2.505, $p$ = 0.0186, Figure 3G-I).

After subthreshold-dosed administration of cocaine, c-Fos staining (n = 12, $t$ = 3.624, $p$ = 0.0047, Figure 3J) and dendritic spine density of virus transfected mPFC pyramidal neurons (n = 6, $t$ = 7.123, $p$ = 0.0021, Figure 3K) were at lower levels in ACE-$C_{OE}$ mice than that in ACE-$C_{Ctrl}$ mice. In parallel, levels of ratio of p-ERK to ERK (n = 6, $t$ = 3.503, $p$ = 0.0248), p-ERK (n = 6, $t$ = 9.063, $p$ = 0.0008), and BDNF (n = 6, $t$ = 8.598, $p$ = 0.0010) were significantly decreased, but levels of ERK (n = 6, $t$ = 0.1728, $p$ = 0.8712), ratio of p-CREB to CREB (n = 6, $t$ = 0.2185, $p$ = 0.8377), p-CREB (n = 6, $t$ = 1.747, $p$ = 0.1556), and CREB (n = 6, $t$ = 1.263, $p$ = 0.2752) were not changed in mPFC by DUSP1 OE virus, when compared to Ctrl virus group (Figure 3L).

**Knockdown of DUSP1 produces cocaine-induced CPP behaviors and increases mPFC activity in ACE mice of adulthood**

To further confirm the role of mPFC DUSP1 in cocaine-preferred behaviors in ACE mice, *AAV9-CaMKII-DUSP1-RNAi-EGFP* (KD virus) and *AAV9-CaMKII-EGFP* (Ctrl virus) were bilaterally infused into mPFC, especially to Cg1 and PrL, to knockdown DUSP1 in pyramidal neurons of mPFC (Figure 4A-B). As shown in Figure 4C, above 70% CaMKII-positive pyramidal neurons within injection sites were transfected with virus. Compared to ACE-C mice with Ctrl virus (ACE-$C_{Ctrl}$ mice), mPFC levels of mRNA (n = 8, $t$ = 9.250, $p$ < 0.0001, Figure 4D), protein (n = 6, $t$ = 11.00, $p$ = 0.0004,

Figure 4E) and activity (n = 11, $t$ = 3.256, $p$ = 0.0099, Figure 4F) of DUSP1 were all much lower in ACE-C mice with KD virus (ACE-$C_{KD}$ mice) after cocaine CPP test. Further, subthreshold-dosed administration of cocaine produced cocaine-preferred behaviors in both ACE-$C_{Ctrl}$ mice (n = 7, $t$ = 2.839, $p$ = 0.0236) and ACE-$C_{KD}$ mice (n = 11, $t$ = 7.104, $p$ < 0.0001), accompanied by higher ΔCPP score in ACE-$C_{OE}$ mice with controls (n = 18, $t$ = 2.211, $p$ = 0.0419, Figure 4G-I).

After subthreshold-dosed administration of cocaine, c-Fos staining (n = 16, $t$ = 4.744, $p$ = 0.0003, Figure 4J) and dendritic spine density of virus transfected mPFC pyramidal neurons (n = 6, $t$ = 5.713, $p$ = 0.0046, Figure 4K) were at higher levels in ACE-$C_{KD}$ mice than that in ACE-$C_{Ctrl}$ mice. In parallel, levels of ratio of p-ERK to ERK (n = 6, $t$ = 3.342, $p$ = 0.0288) were increased, level of p-CREB (n = 6, $t$ = 3.411, $p$ = 0.0270) were decreased, and levels of p-ERK (n = 6, $t$ = 2.125, $p$ = 0.1008), ERK (n = 6, $t$ = 0.1856, $p$ = 0.8618), ratio of p-CREB to CREB (n = 6, $t$ = 0.9360, $p$ = 0.4023), CREB (n = 6, $t$ = 2.041, $p$ = 0.1109) and BDNF (n = 6, $t$ = 0.5882, $p$ = 0.5880) were not changed in mPFC by DUSP1 KD virus, when compared to Ctrl virus group (Figure 4L).

**Discussion**

The current study found that adolescent cocaine exposure (ACE) enhanced the sensitivity of mice to cocaine in their adulthood, as indicated by significant cocaine-preferred behaviors in ACE mice. By mapping brain activity in response to subthreshold doses of cocaine, we found that mPFC, especially glutamatergic neurons of Cg1 and PrL, was obviously activated in ACE mice, indicating that mPFC activity is closely associated with the ACE-increased sensitivity to drugs in later life of mice. By screening mPFC transcriptome, we found that *Dusp1* gene and the genes related to MAPK signals pathway were significantly upregulated in mPFC of cocaine-preferred

mice with ACE experiences. By contrast, the level and activity of mPFC DUSP1 protein were attenuated in response to cocaine in ACE mice of adulthood. In order to investigate the roles of converse phenotypes of DUSP1 mRNA and protein in response to cocaine, both local overexpression and knockdown of mPFC DUSP1 were performed in ACE mice. We found that specific overexpression of DUSP1 on glutamatergic neurons of mPFC efficiently blocks cocaine-induced CPP behaviors in ACE mice, indicating that mPFC DUSP1 is key regulator underlying ACE-enhanced sensitivity to drugs. Further, we found that overexpression of DUSP1 reduced, while knockdown of DUSP1 triggered mPFC activation by subthreshold doses of cocaine in ACE mice, accompanied with a negatively regulated phosphorylation of ERK1/2 in mPFC (Figure 5).

Adolescence is a critical period of brain development and maturation so that makes the adolescent brain highly susceptible to neurotoxicity of drugs. Exposure to Δ9-tetrahydrocannabinol (psychoactive ingredient of cannabis) enhanced sensitivity to cocaine in rats even into adulthood (34), and adolescent methylphenidate use (psychostimulant drug to treat attention deficit hyperactivity disorder) increased reactivity and vulnerability to cocaine in rats of adulthood (35), suggesting that adolescent use of the psychostimulant is an important risk factor for addiction susceptibility in later life. Previously using the similar ACE mice models with this study, we found that there was no differences on acquisition, extinction and reinstatement of CPP behaviors by repeated exposure to addictive doses of cocaine (15 mg/kg) in adulthood between ACE mice and controls (16). However, here we found that subthreshold dosed administration of cocaine (1 mg/kg) effectively induced cocaine-preferred behaviors in ACE mice but not in control mice of their adulthood, indicating that ACE increase the sensitivity to cocaine which may render adult mice more

susceptible to cocaine. Cass et.al (36) found that adolescent cocaine administration produced mPFC disinhibition that endured throughout adulthood. Our previous studies found that adolescent cocaine exposure induced prolonged modifications on synapses (17) and triggered neuronal activation (16) in mPFC of adult rodents, which contribute to the increased anxiety-like behaviors in later life. Here, by mapping the activation of potential brain regions involved in the increased sensitivity to cocaine, we found that mPFC, especially glutamatergic neurons in Cg1 and PrL, were obviously and strongly evoked in response to cocaine challenge in adult ACE mice. These findings suggest that ACE-induced plastic changes in mPFC play critical roles in facilitation of susceptibility to drugs in later life. Previously, we found that ACE suppressed mPFC activity partially through enhancing local GABAergic transmission on mPFC pyramidal neurons (16) and reduced dendritic spines of mPFC pyramidal neurons (17) in adulthood. However, unlike baseline condition, here we found that cocaine challenge in adulthood activated more glutamatergic neurons but did not change GABAergic including its subtypes of PV-positive and SOM-positive neurons in mPFC, and increased dendritic spines of mPFC pyramidal neurons in ACE mice of adulthood. Based on these results, we hypothesized that the cocaine-changed signals in glutamatergic neurons of mPFC should be the mechanic basis for mPFC activation and susceptibility behavior in ACE mice of adulthood.

In order to screen key signals, mPFC transcriptome was performed after cocaine administration in adult mice. We found that *Dusp1* gene and genes related to mitogen-activated protein kinase phosphatases (MAKPs) pathway were obviously upregulated in mPFC after cocaine challenge in ACE mice. While, level and activity of DUSP1 protein were decreased at the same time. We believe that the inconsistency between gene and protein changes of DUSP1 is due to their different meanings reflected in

response to cocaine challenge. Takaki et al. (37) reported that *Dusp1* mRNA levels were significantly increased after acute or chronic methamphetamine administration in PFC of animals. We thought that the increased *Dusp1* gene in response to cocaine challenge, similar to immediate early genes of *c-fos*, *Jun*, *Ark*, reflected rapid and sensitive response of mPFC to cocaine in ACE mice, further indicating the important involvement of mPFC in process of susceptibility to drugs. In contrast, we found that the decreased DUSP1 protein level and activity was consistent with upregulated genes in MAPK-related signals by transcriptome analysis in mPFC of ACE mice by cocaine challenge during adulthood. Thus, DUSP1 protein might be key regulatory molecule to plastic changes in mPFC which underlies the increased sensitivity to drugs in ACE mice of adulthood. Indeed, we found that specific overexpression but not knockdown of DUSP1 on glutamatergic neurons of mPFC efficiently suppressed cocaine-activated mPFC, and ultimately reduced cocaine-preferred behaviors in ACE mice. As a negative regulatory factor on MAPK-related signals, DUSP1 is also known as MKP-1. By dephosphorylating p38, JNKs and ERK (38), DUSP1 regulates the brain function. Among them, ERK-related signals are well-studied in cocaine addiction. The ERK signaling pathway is a canonical MAPK signaling pathway that has been implicated in synaptic plasticity and neuronal growth (39). Acute cocaine administration is sufficient to increased phosphorylation of ERK in PFC, which contribute to the long-term plastic changes by cocaine in the brain (40-42). While, blockade of ERK activation during re-exposure to cocaine erased previously cocaine-preferred behaviors (43). In the present study, we found that levels of p-ERK increased when cocaine-elicited mPFC, while it was decreased in DUSP1-overexpressed mPFC with reduced activity in ACE mice, suggesting that DUSP1 may recruit ERK-related signals to regulate mPFC activity, and therefore influence sensitivity to cocaine challenge in ACE mice. In the future study,

the mechanistic investigation of DUSP1/MAPK signal pathway underlying the phenotypes of higher cocaine-preferred behaviors should be further explored in ACE mice.

Collectively, our findings reveals a novel signal mechanism of DUSP1 / ERK1/2 / mPFC activation underlying higher sensitivity to drugs caused by adolescent experiences of drug abuse, suggesting that targeting mPFC DUSP1 may represent a promising therapeutic strategy for preventing drug addiction, particularly in addicts with a history of adolescent drugs exposure.

## Materials and methods

### Animals

Male C57BL/6 wild type (WT) mice weighing 12-15 g were used. All animals were housed at constant humidity (40~60%) and temperature (24 ± 2 ℃) with a 12-hour light/dark cycle (lights on at 8 a.m.) and allowed free access to food and water. All mice were handled for three days before onset of experiments. All procedures were carried out in accordance with the National Institutes of Health Guide for the Care and Use of Laboratory Animals and approved by the Institutional Animal Care and Use Committee (IACUC) at Nanjing University of Chinese Medicine.

### Drug treatment

From postnatal day 28 (P28) to P42, male C57BL/6 WT mice were assigned to receive cocaine hydrochloride (15 mg/kg, dissolved in saline, i.p., Qinghai Pharmaceutical, China) or saline (0.2 mL, i.p.) once daily for 15 consecutive days. From P43-P74, these mice were kept at their home cage (four mice one cage). From P75 to P78, a subset of mice were subjected to conditioned place preference (CPP) training and test induced by subthreshold dose of cocaine hydrochloride (1 mg/kg, Figure 1A).

## CPP

One cohort of mice were subjected to CPP training and test on P78. The CPP test was performed in the TopScan3D CPP apparatus (CleverSys, VA, USA), which is constructed of two distinct chambers (15 × 15 × 23 cm each) separated by a removable guillotine door. The CPP procedure consisted of three phases: the pre-conditioning test (Pre-test, P75), conditioning (CPP training, P76-77) and post-conditioning test (Test, P78). Here, subthreshold doses of cocaine (1 mg/kg), which is believed not enough to induce CPP behaviors in naïve mouse, were used to induced CPP behaviors. During CPP training, mice were injected with saline (0.2 mL, i.p.) in the morning and cocaine (1 mg/kg, i.p.) in the afternoon once daily. After each injection, the mice were confined to one chamber (non-drug-paired chamber or drug-paired chamber) for 45 min. During the Pre-test and Test, mice freely access two chambers for 15 min. The CPP score is the time spent in drug-paired chamber minus that in non-drug-paired chamber, and the ΔCPP score is the test CPP score minus the pre-test CPP score.

## Immunofluorescence

On P78, brain tissue were collected from a subset of mice within 90 min after CPP test. Mice brains were perfused with 4% paraformaldehyde (PFA). The coronal brain sections (30 μm) were cut on a cryostat (Leica, Germany). The sections were incubated in 0.3% (v/v) Triton X-100 for 0.5 h, blocked with 5% donkey serum for 1.5 h at room temperature, and incubated overnight at 4 ℃ with the following primary antibodies: rabbit anti-c-Fos (1:1500, RRID: AB_2247211, Cell Signalling Technology, USA), mouse anti-NeuN (1:800, RRID: AB_2298772, Millipore, USA), DUSP1 (1:100, BM4856, Boster Biotechnology, China), mouse anti-GAD67 (1:500, RRID: AB_2278725, Millipore, USA), mouse anti-PV (1:250, BM1339, Boster Biotechnology, China), mouse anti-SOM (1:50, RRID:AB_2271061, Santa Cruz,

USA), mouse anti-CaMKIIα (1:100, SC-13141, Santa Cruz, USA) and mouse anti-CaMKIIα (1:200, RRID: AB_2721906, Cell Signalling Technology, USA), followed by the corresponding fluorophore-conjugated secondary antibodies for 1.5 h at room temperature. The following secondary antibodies were used here: Alexa Fluor 555-labeled donkey anti-rabbit secondary antibody (1:500, RRID: AB_2762834, Invitrogen, USA), Alexa Fluor 488-labeled donkey anti-mouse secondary antibody (1:500, RRID: AB_141607, Invitrogen, USA). Fluorescence signals were visualized using a Leica DM6B upright digital research microscope (Leica, Germany) or Leica TCS SP8 (Leica, Germany).

**Fiber photometry**

On P51, the rAAV2/9-CaMKII-GCaMp6m (PT-0111, 3.24E+12 vg/ml, Brain VTA, China) virus was bilaterally injected into mPFC (AP + 2.10 mm, ML ± 0.3 mm, DV – 2.15 mm), especially into PrL of mice. On P78, the GCaMp6m signals in mPFC were recorded during CPP test. An optical fiber (200 μm outer diameter, 0.37 numerical aperture, Inper Ltd., China) was placed 100 μm above the viral injection site. The calcium-dependent fluorescence signals were obtained by stimulating cells that transfected GCaMp6m virus with a 470 nm LED (35-40 μW at fiber tip), while calcium-independent signals were obtained by stimulating these cells with a 405 nm LED (15-20 μW at fiber tip). The LED lights of 470 nm and 405 nm were alternated at 66 fps and light emission was recorded using sCMOS camera containing the entire fiber bundle (2 m in length, NA = 0.37, 200 μm core, Inper Ltd.). The analog voltage signals fluorescent was filtered at 30 Hz and digitalized at 100 Hz. The GCaMp6m signals were recorded and analyzed by Inper Studio Multi Color EVAL15 software (Inper Ltd., China) and Inper Data Process V0.5.9 (Inper Ltd., China), respectively. F0 is the baseline fluorescence signal which was recorded for 1 sec before mice entering into the

cocaine-paired chamber. F is the real-time fluorescence signal which was recorded for 4 sec after mice entering into the cocaine-paired chamber during CPP test. Each recording trail was with 5 sec recording duration. The values of ΔF/F are calculated by (F-F0)/F0. The area under curve (AUC) is the integral under recording duration related to corresponding baseline at every trial.

**Dendritic spine analysis**

The dendritic spines of CaMKII-positive neurons in mPFC were stained by virus tagged with CaMKII promotors used in the present study. On P78, the dendritic spines were photographed and quantified using the z-stack scanning function of Leica TCS SP8 confocal microscope (Leica, Germany) and LAS X software (Leica, Germany), respectively. The density of spines was counted in about 50 μm dendritic segments from the second and third branches of CaMKII-positive neurons in length.

**The mRNA sequencing and data processing in mPFC**

On P78, mPFC tissue were collected from mice after CPP test. Library preparation was performed by Novogene Bioinformatics Technology Co., Ltd (China). RNA degradation and purity were monitored on 1% agarose gels and using the NanoPhotometer ® spectrophotometer (IMPLEN, CA, USA). RNA integrity was assessed using the RNA Nano 6000 Assay Kit of the Bioanalyzer 2100 system (Agilent Technologies, CA, USA). The mRNA was purified and fragmented from a total amount of 1 μg RNA per sample. cDNA was synthesized, adenylated and ligated with hairpin-structured NEBNext Adaptor before hybridization. 250-300 bp cDNA fragments were purified and preferentially selected for hybridization. The PCR products were purified (AMPure XP system) and library quality was assessed on the Agilent Bioanalyzer 2100 system. Index-coded samples were clustered on a cBot Cluster Generation System

using TruSeq PE Cluster Kit v3-cBot-HS (Illumia) and sequenced on an Illumina Novaseq platform. Differential mRNA expression analysis was performed using the DESeq2 R package (1.16.1). The *p* values were adjusted using the Benjamini & Hochberg method. Cutoffs of an absolute fold change > 1 and a correlated *p* value < 0.05 were set for significantly differential expression. The Bioinformatics analysis, including GO, KEGG and Protein-Protein Interaction (PPI) of upregulated genes by subthreshold doses of cocaine in ACE mice were performed in this study.

**RNA extraction and quantitative real-time PCR**

On P78, brain tissue were collected from a subset of mice within 90 min after CPP test. The mPFC tissue were dissected immediately on dry ice. Total RNA was extracted from mPFC using FastPure Cell/Tissue Total RNA Isolation Kit (Vazyme, China). After RNA extraction, the amount of RNA was normalized across samples, and cDNA was created using Vazyme (HiScript II Q RT SuperMix for Qpcr (+gDNA wiper)). The β-actin was used as the internal control. The primers of DUSP1 and β-actin were as follows: DUSP1 (forward, GTTGTTGGATTGTCGCTCCTT; reverse, TTGGGCACGATATGCTCCAG), β-actin (forward, GGCTGTATTCCCCTCCATCG; reverse, CCAGTTGGTAACAATGCCATGT). DUSP1 mRNA levels were normalized to β-actin mRNA levels. The relative mRNA level was calculated by the comparative CT method ($2^{-\Delta\Delta Ct}$).

**Western blot**

On P74 and P78, brain tissue were collected from two subsets of mice without CPP training (P74) or within 90 min after CPP test (P78). The mPFC tissue were dissected immediately on dry ice. Total mPFC protein was extracted using RIPA lysis buffer (Shanghai Beyotime, China). Protein samples (15 μg) was separated by 10% SDS–

PAGE or 12% SDS–PAGE and electrophoretically transferred onto PVDF membranes. The transferred membranes were blocked with 5% non-fat dry milk and 0.1% Tween 20 in 10 mM Tris–HCl (TBST buffer, pH 7.5) for 1.5 h at room temperature, then subsequently incubated with the following primary antibodies: c-Fos (1:1500, Rabbit, RRID: AB_2247211, Cell Signalling Technology, USA), DUSP1 (1:1000 , Rabbit, BM4856, Boster Biotechnology, China), $ERK_{1/2}$ (1:1000, Rabbit, BM4326, Boster Biotechnology, China), p-$ERK_{1/2}$ (1:1000, Rabbit, BM4156, Boster Biotechnology, China), CREB (1:1000, Rabbit, RRID:AB_331277, Cell Signaling Technology, USA), p-CREB (1:1000, Rabbit, RRID:AB_2561044, Cell Signaling Technology, USA), BDNF (1:1000, Mouse, RRID:AB_2881675, Proteintech, USA). The next day, the membranes were washed three times in Tris-buffered saline with Tween 20 (TBS-T) and incubated with horseradish peroxidase (HRP)-conjugated secondary antibody goat anti-rabbit (1:5000, RRID:AB_2814709, Beijing ComWin Biotech Co., China) or goat anti mouse (1:5000, RRID:AB_2736997, Beijing ComWin Biotech Co., China) at room temperature for 1 h. The blots were visualized by the ECL kit (Beijing ComWin Biotech Co., China) and the signal was visualized by imaging system (Tanon-5200, Shanghai, China). The blots were washed with stripping buffer (Beyotime Institute of Biotechnology) to allow reprobing with other antibodies. In this study, β-actin was used as control. Values for target protein levels were calculated using Image J software (NIH, USA). The relative level of each protein was normalized to β-actin.

**Total dual specificity phosphatase 1 (DUSP1) measurement in mPFC by ELISA**

On P74 and P78, brain tissue were collected from two subsets of mice without CPP training (P74) or within 90 min after CPP test (P78). The mPFC tissue were dissected

immediately on dry ice. The activity of mPFC DUSP1 was measured by commercial ELISA (Mouse Dual Specificity Phosphatase 1 (DUSP1) ELISA Kit instruction, Shanghai shyx-bio.com, China). The mPFC tissues were diluted 1:10 in saline and mashed using Tissue Grinder (Wuhan Servicebio technology CO., China), then centrifugated for 30 minutes at 3000×g at 2-8℃ and the supernatants were store samples at -20℃. The 50 μL mixture of sample and Sample Diluent (1:4) were put in one well of plate. Then, add 100 μL of HRP-conjugate reagent to each well, cover with an adhesive strip and incubate for 60 minutes at 37 ℃. Washing the wells with Wash Solution (400 μL) five times. Then, added chromogen solution A 50 μL and chromogen solution B 50 μL to each well and incubated for 15 minutes at 37 ℃. The reaction was stopped by adding 50 μL Stop Solution. Read the Optical Density (O.D.) at 450 nm using a standard microplate reader (BIO-RAD iMark Microplate Reader, USA) within 15 minutes.

**Specific overexpression or knockdown of DUSP1 on CaMKII-positive neurons in mPFC**

On P51, four cohorts of mice were anesthetized with 2% isoflurane in oxygen, and were fixed in a stereotactic frame (RWD, China). A heating pad was used to maintain the core body temperature of the animals at 36 ℃. The coordinates of mPFC were AP + 2.10, ML ± 0.3, DV – 2.15 in mm. In Experiment of overexpression of DUSP1, a volume of 400 nL of CaMKIIap-MCS-EGFP-3Flag-SV40 PloyA (AAV9-CaMKIIap-DUSP1-RNAOE-EGFP, 4.90E+13v.g/ml; Cat#: GOSV0322969, Gene Chem, China) or CaMKIIap-EGFP-SV40 PloyA (AAV9-CaMKIIap-EGFP, 4.01E+12v.g/ml; Cat#: AAV9/CON540, Gene Chem, China) bilaterally into the mPFC (AP + 2.10 mm, ML ± 0.3 mm, DV – 2.15 mm) at a rate of 80 nL/min. In Experiment of knockdown of DUSP1,

a volume of 400 nL of CaMKIIap-EGFP-MIR155(MCS)-SV40 PloyA (AAV9-CaMKIIap-DUSP1-RNAi-EGFP, 1.10E+13 v.g/ml; Cat#: GIDV0295686, Gene Chem, China) or CaMKIIap-EGFP-SV40 PloyA (AAV9-CaMKIIap-EGFP, 4.01E+12v.g/ml; Cat#: AAV9/CON540, Gene Chem, China) bilaterally into the at a rate of 80 nL/min. After surgery, mice were maintained at home cage about 3 weeks.

**Statistical analysis**

Statistical analysis was carried out using GraphPad Prism 8.0.2 software. All data are presented as the Mean ± SEM. The data of CPP score between ASE-C and ACE-C groups are analyzed by two-way analysis of variance (ANOVA), while CPP score between Pre-test and Test in each mouse were analyzed by paired *t*-tests. Other data were analyzed by unpaired *t*-tests. GO and KEGG enrichment analysis of differentially expressed genes was implemented by the clusterProfiler R package, and a corrected $p < 0.05$ were considered as significantly enriched. The Protein-Protein Interaction (PPI) network was drawn via the cytoscape 3.4.0 analysis software. All statistical significance was set as $p < 0.05$.

**Author contribution**

Wei X and Cheng Z have equal contribution to the manuscript. Wei X, Cheng Z, Fan Y and Chang J performed behavioral tests, morphological tests and virus-related experiment. Chen W, Guo H, Liu Z, Hu T, Zhang Y and Cai Q assist the data analysis. Fan Y, Chang J and Ge F performed data analysis. Guan X and Fan Y wrote the manuscript. Guan X developed the overall concept.

**Acknowledgment**

This work is supported by National Natural Science Foundation of China (82071495), Natural Science Foundation of Jiangsu Province, China (BK20201398) and Natural

Science Foundation of the Higher Education Institutions of Jiangsu Province, China (21KJB360007).

**Conflict of interests**

The authors have no conflict of interests to declare.

**Data availability statement**

The data that support the findings of this study are available from the corresponding author upon reasonable request.

## Reference


1. Chambers RA, et al. Developmental neurocircuitry of motivation in adolescence: a critical period of addiction vulnerability. *The American journal of psychiatry.* 2003;160(6):1041-52.
2. Paule MG. Chronic drug exposures during development in nonhuman primates: models of brain dysfunction in humans. *Frontiers in bioscience : a journal and virtual library.* 2005;10(2240-9.
3. Spear LP. Consequences of adolescent use of alcohol and other drugs: Studies using rodent models. *Neuroscience and biobehavioral reviews.* 2016;70(228-43.
4. Wong WC, and Marinelli M. Adolescent-onset of cocaine use is associated with heightened stress-induced reinstatement of cocaine seeking. *Addiction biology.* 2016;21(3):634-45.
5. Jordan CJ, and Andersen SL. Sensitive periods of substance abuse: Early risk for the transition to dependence. *Developmental Cognitive Neuroscience.* 2017;25(29-44.
6. Giedd JN. Structural magnetic resonance imaging of the adolescent brain. *Ann N Y Acad Sci.* 2004;1021(77-85.
7. Koss WA, et al. Dendritic remodeling in the adolescent medial prefrontal cortex and the basolateral amygdala of male and female rats. *Synapse.* 2014;68(2):61-72.
8. Shapiro LP, et al. Differential expression of cytoskeletal regulatory factors in the adolescent prefrontal cortex: Implications for cortical development. *J Neurosci Res.* 2017;95(5):1123-43.
9. Reynolds LM, et al. Amphetamine in adolescence disrupts the development of medial prefrontal cortex dopamine connectivity in a DCC-dependent manner. *Neuropsychopharmacology : official publication of the American College of Neuropsychopharmacology.* 2015;40(5):1101-12.
10. Perry JL, et al. Prefrontal cortex and drug abuse vulnerability: translation to prevention and

treatment interventions. *Brain Res Rev.* 2011;65(2):124-49.

11. Zhang Y, et al. Molecular changes in the medial prefrontal cortex and nucleus accumbens are associated with blocking the behavioral sensitization to cocaine. *Scientific reports.* 2015;5(1):16172.

12. Caffino L, et al. A single cocaine administration alters dendritic spine morphology and impairs glutamate receptor synaptic retention in the medial prefrontal cortex of adolescent rats. *Neuropharmacology.* 2018;140(209-16.

13. Caffino L, et al. A single cocaine exposure disrupts actin dynamics in the cortico-accumbal pathway of adolescent rats: modulation by a second cocaine injection. *Psychopharmacology.* 2017;234(8):1217-22.

14. Chocyk A, et al. Early-life stress affects the structural and functional plasticity of the medial prefrontal cortex in adolescent rats. *The European journal of neuroscience.* 2013;38(1):2089-107.

15. Fuhrmann D, et al. Adolescence as a Sensitive Period of Brain Development. *Trends in cognitive sciences.* 2015;19(10):558-66.

16. Shi P, et al. Adolescent cocaine exposure enhances the GABAergic transmission in the prelimbic cortex of adult mice. *FASEB journal : official publication of the Federation of American Societies for Experimental Biology.* 2019;33(7):8614-22.

17. Zhu W, et al. Adolescent cocaine exposure induces prolonged synaptic modifications in medial prefrontal cortex of adult rats. *Brain structure & function.* 2018;223(4):1829-38.

18. Vertes RP. Differential projections of the infralimbic and prelimbic cortex in the rat. *Synapse.* 2004;51(1):32-58.

19. Passetti F, et al. The frontal cortex of the rat and visual attentional performance: dissociable functions of distinct medial prefrontal subregions. *Cerebral cortex (New York, NY : 1991).* 2002;12(12):1254-68.

20. Taber MT, and Fibiger HC. Electrical stimulation of the prefrontal cortex increases dopamine release in the nucleus accumbens of the rat: modulation by metabotropic glutamate receptors. *The Journal of neuroscience : the official journal of the Society for Neuroscience.* 1995;15(5 Pt 2):3896-904.

21. Sesack SR, et al. Topographical organization of the efferent projections of the medial prefrontal cortex in the rat: an anterograde tract-tracing study with Phaseolus vulgaris leucoagglutinin. *The Journal of comparative neurology.* 1989;290(2):213-42.

22. Kawaguchi Y. Groupings of nonpyramidal and pyramidal cells with specific physiological and morphological characteristics in rat frontal cortex. *Journal of neurophysiology.* 1993;69(2):416-31.

23. Kawaguchi Y, and Kubota Y. Correlation of physiological subgroupings of nonpyramidal cells with parvalbumin- and calbindinD28k-immunoreactive neurons in layer V of rat frontal cortex. *Journal of neurophysiology.* 1993;70(1):387-96.

24. Pierce RC, et al. Ibotenic acid lesions of the dorsal prefrontal cortex disrupt the expression of behavioral sensitization to cocaine. *Neuroscience.* 1998;82(4):1103-14.

25. Williams JM, and Steketee JD. Cocaine increases medial prefrontal cortical glutamate overflow in cocaine-sensitized rats: a time course study. *The European journal of neuroscience.* 2004;20(6):1639-46.

26. Low HB, and Zhang Y. Regulatory Roles of MAPK Phosphatases in Cancer. *Immune network.*

2016;16(2):85-98.

27. Xia L, et al. Rosiglitazone Improves Glucocorticoid Resistance in a Sudden Sensorineural Hearing Loss by Promoting MAP Kinase Phosphatase-1 Expression. *Mediators of inflammation.* 2019;2019(7915730.

28. Taylor DM, et al. MAP kinase phosphatase 1 (MKP-1/DUSP1) is neuroprotective in Huntington's disease via additive effects of JNK and p38 inhibition. *The Journal of neuroscience : the official journal of the Society for Neuroscience.* 2013;33(6):2313-25.

29. Xu P, et al. DUSP1 alleviates cerebral ischaemia reperfusion injury via inactivating JNK-Mff pathways and repressing mitochondrial fission. *Life Sci.* 2018;210(251-62.

30. Ndong C, et al. Mitogen activated protein kinase phosphatase-1 prevents the development of tactile sensitivity in a rodent model of neuropathic pain. *Molecular pain.* 2012;8(34.

31. Jefsen OH, et al. Transcriptional regulation in the rat prefrontal cortex and hippocampus after a single administration of psilocybin. *Journal of Psychopharmacology.* 2020;35(4):483-93.

32. Wojcieszak J, et al. Induction of immediate early genes expression in the mouse striatum following acute administration of synthetic cathinones. *Pharmacological Reports.* 2019;71(6):977-82.

33. Spear LP. The adolescent brain and age-related behavioral manifestations. *Neuroscience and biobehavioral reviews.* 2000;24(4):417-63.

34. Friedman AL, et al. Effects of adolescent Δ9-tetrahydrocannabinol exposure on the behavioral effects of cocaine in adult Sprague-Dawley rats. *Experimental and clinical psychopharmacology.* 2019;27(4):326-37.

35. Brandon CL, et al. Enhanced reactivity and vulnerability to cocaine following methylphenidate

treatment in adolescent rats. *Neuropsychopharmacology : official publication of the American College of Neuropsychopharmacology.* 2001;25(5):651-61.

36. Cass DK, et al. Developmental disruption of gamma-aminobutyric acid function in the medial prefrontal cortex by noncontingent cocaine exposure during early adolescence. *Biological psychiatry.* 2013;74(7):490-501.

37. Takaki M, et al. Two kinds of mitogen-activated protein kinase phosphatases, MKP-1 and MKP-3, are differentially activated by acute and chronic methamphetamine treatment in the rat brain. *Journal of neurochemistry.* 2001;79(3):679-88.

38. Lawan A, et al. Skeletal Muscle–Specific Deletion of MKP-1 Reveals a p38 MAPK/JNK/Akt Signaling Node That Regulates Obesity-Induced Insulin Resistance. *Diabetes.* 2018;67(4):624-35.

39. Sweatt JD. The neuronal MAP kinase cascade: a biochemical signal integration system subserving synaptic plasticity and memory. *Journal of neurochemistry.* 2001;76(1):1-10.

40. Valjent E, et al. Addictive and non-addictive drugs induce distinct and specific patterns of ERK activation in mouse brain. *The European journal of neuroscience.* 2004;19(7):1826-36.

41. Radwanska K, et al. Regulation of cocaine-induced activator protein 1 transcription factors by the extracellular signal-regulated kinase pathway. *Neuroscience.* 2006;137(1):253-64.

42. Sun WL, et al. Molecular Mechanism: ERK Signaling, Drug Addiction, and Behavioral Effects. *Progress in molecular biology and translational science.* 2016;137(1-40.

43. Valjent E, et al. Inhibition of ERK pathway or protein synthesis during reexposure to drugs of abuse erases previously learned place preference. *Proceedings of the National Academy of Sciences of the United States of America.* 2006;103(8):2932-7.

## Figure legends

**Figure 1. Subthreshold-dosed administration of cocaine elicits cocaine CPP behaviors and triggers mPFC activity in ACE mice of adulthood. A,** Experimental models and timeline. **B,** CPP score. **C,** ΔCPP score. **D,** Heatmap of spent duration by mice in CPP apparatus. **E,** C-Fos staining after CPP test in mPFC and its subregions of Cg1, PrL, IL. The c-Fos (red) and NeuN (green) are used as markers for evaluating cell activity and labeling neuron, respectively. Scale bar, 400 μm/100 μm. **F,** Dendritic spine density of pyramidal neurons in mPFC. Scale bar, 10 μm. **G,** Schematic diagram of viral injection. **H,** CPP score. **I,** ΔCPP score. **J,** Heatmap of spent duration by mice in CPP apparatus. **K,** Heatmap of GCaMp6m fluorescence at first 4 sec when mice entering cocaine-paired chamber. **L,** Quantification of ΔF/F. **M,** The AUC of ΔF/F. Cg1, cingulate cortex; PrL, prelimbic cortex; IL, infralimbic cortex; ASE-C, subthreshold-dosed administration of cocaine in adolescent saline-exposed mice; ACE-C, subthreshold-dosed administration of cocaine in adolescent cocaine-exposed mice; N.S., $p > 0.05$, $^{\#}$, $p < 0.05$, $^{\#\#}$, $p < 0.01$ vs baseline (pre-test CPP score); N.S., $p > 0.05$, *, $p < 0.05$, **, $p < 0.01$ vs ASE-C mice.

**Figure 2. Subthreshold-dosed administration of cocaine increases *Dusp1* gene but decreases DUPS1 protein and activity in mPFC of adult ACE mice. A,** *Dusp1* mRNA levels on P78. **B,** DUSP1 protein levels and activity on P78. **C,** DUSP1 activity on P78. **D,** DUSP1 staining in CaMKII-positive neurons. Scale bar, 400 μm/100 μm. **E,** Levels of MAPK-related signal proteins on P78, including p-ERK/ERK, p-ERK, ERK, p-CREB/CREB, p-CREB, CREB and BDNF. ASE-C, subthreshold-dosed administration of cocaine in adolescent saline-exposed mice; ACE-C, subthreshold-dosed administration of cocaine in adolescent cocaine-exposed mice; N.S., $p > 0.05$, *, $p < 0.05$, **, $p < 0.01$ vs ASE-C mice.

**Figure 3. Overexpression of mPFC DUSP1 blocks cocaine-induced CPP behaviors and attenuates mPFC activity in ACE mice of adulthood. A,** Experimental design and timeline. **B,** Schematic diagram of viral injection. Scale bar, 400 μm. **C,** Percentage of viral transfected neurons in CaMKII-positive neurons of mPFC. Scale bar, 200 μm/100 μm. **D,** *Dusp1* mRNA levels on P78. **E,** DUSP1 protein levels on P78. **F,** DUSP1 activity on P78. **G,** CPP score. **H,** ΔCPP score. **I,** Heatmap of spent duration by mice in CPP apparatus. **J,** C-Fos-stained value in virus-transfected neurons. Scale bar, 200 μm/100 μm. **K,** Dendritic spine density of pyramidal neurons in mPFC. Scale bar, 10 μm. **L,** Levels of MAPK-related signal proteins, including p-ERK/ERK, p-ERK, ERK, p-CREB/CREB, p-CREB, CREB and BDNF. ACE-$C_{Ctrl}$, ACE-C mice injected with Ctrl virus; ACE-$C_{OE}$, ACE-C mice with overexpression virus of DUSP1; N.S., $p > 0.05$, *, $p < 0.05$, **, $p < 0.01$ vs ACE-$C_{Ctrl}$ mice.

**Figure 4. Knockdown of DUSP1 maintains cocaine-preferred behaviors and increases mPFC activity in ACE mice of adulthood. A,** Experimental design and timeline. **B,** Schematic diagram of viral injection. Scale bar, 400 μm. **C,** Percentage of viral transfected neurons in CaMKII-positive neurons of mPFC. Scale bar, 200 μm/100 μm. **D,** *Dusp1* mRNA levels on P78. **E,** DUSP1 protein levels on P78. **F,** DUSP1 activity on P78. **G,** CPP score. **H,** ΔCPP score. **I,** Heatmap of spent duration by mice in CPP apparatus. **J,** C-Fos-stained value in virus-transfected neurons. Scale bar, 200 μm/100 μm. **K,** Dendritic spine density of pyramidal neurons in mPFC. Scale bar, 10 μm. **L,** Levels of MAPK-related signal proteins, including p-ERK/ERK, p-ERK, ERK, p-CREB/CREB, p-CREB, CREB and BDNF. ACE-$C_{Ctrl}$, ACE-C mice injected with Ctrl virus; ACE-$C_{KD}$, ACE-C mice with knockdown virus of DUSP1; N.S., $p > 0.05$, *, $p < 0.05$, **, $p < 0.01$ vs ACE-$C_{Ctrl}$ mice.

**Figure 5. Graphical summary of the present study.** In adulthood, mice with cocaine-

exposed experience during adolescent period (ACE-C mice) exhibits higher sensitivity to cocaine, accompanied by more activated mPFC and lower levels of DUSP1 protein and activity of mPFC in response to subthreshold-dosed administration of cocaine. Specific overexpression of DUSP1 on mPFC glutamatergic neurons efficiently blocks cocaine-preferred behaviors and reduces mPFC activity, while knockdown of DUSP1 maintains cocaine-preferred behaviors and increases mPFC activity in ACE-C mice. It might be through regulating MAPK signal molecules such as ERK1/2 that DUSP1 regulates the enhanced mPFC activation and sensitivity of ACE mice to cocaine.

# Figure1

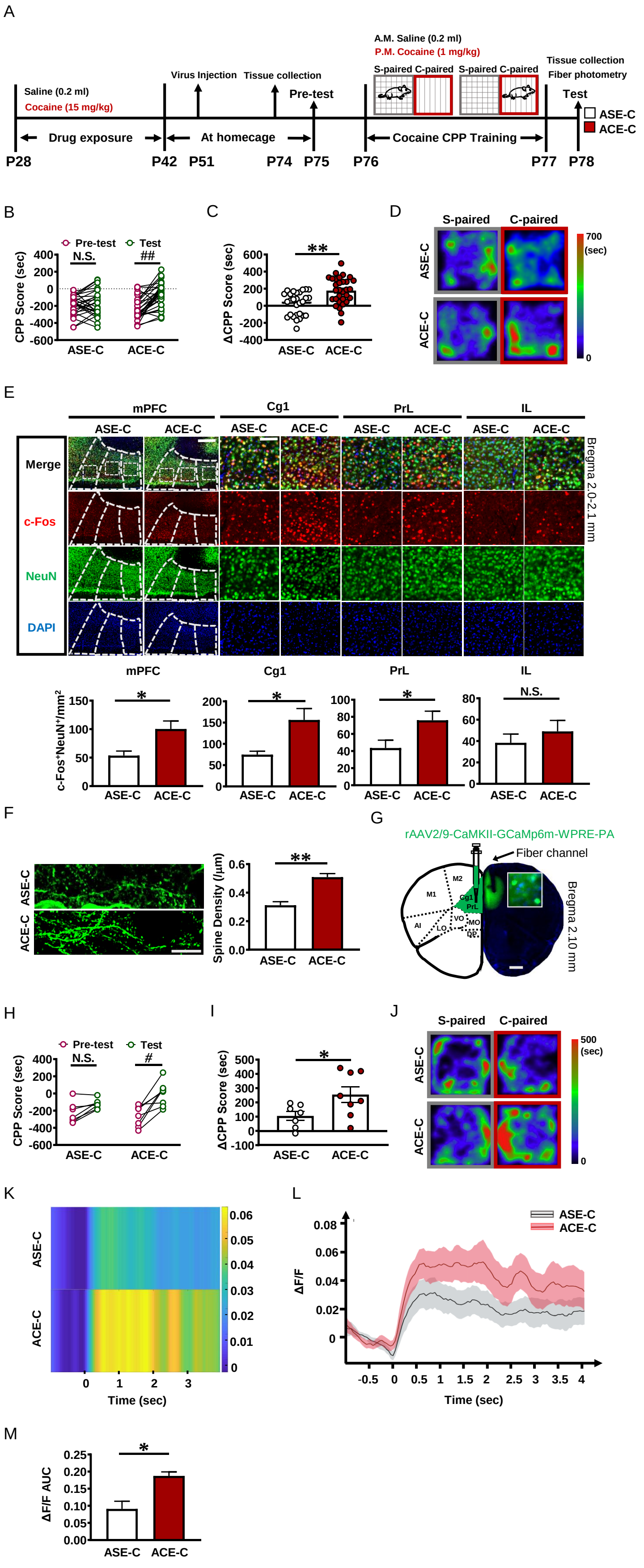
A
A.M. Saline (0.2 ml)
P.M. Cocaine (1 mg/kg)
S-paired C-paired
S-paired C-paired
Tissue collection
Fiber photometry
Virus Injection
Tissue collection
Pre-test
Test
Saline (0.2 ml)
Cocaine (15 mg/kg)
ASE-C
ACE-C
Drug exposure
At homecage
Cocaine CPP Training
P28
P42
P51
P74
P75
P76
P77
P78
B
Pre-test
Test
N.S.
##
CPP Score (sec)
ASE-C
ACE-C
C
**
ΔCPP Score (sec)
ASE-C
ACE-C
D
S-paired
C-paired
ASE-C
ACE-C
700
(sec)
0
E
mPFC
Cg1
PrL
IL
ASE-C
ACE-C
Merge
c-Fos
NeuN
DAPI
Bregma 2.0-2.1 mm
c-Fos+NeuN+/mm2
*
N.S.
F
ASE-C
ACE-C
**
Spine Density (/μm)
G
rAAV2/9-CaMKII-GCaMp6m-WPRE-PA
Fiber channel
M2
M1
Cg1
PrL
AI
VO
LO
MO
DP
Bregma 2.10 mm
H
Pre-test
Test
N.S.
#
CPP Score (sec)
ASE-C
ACE-C
I
*
ΔCPP Score (sec)
ASE-C
ACE-C
J
S-paired
C-paired
ASE-C
ACE-C
500
(sec)
0
K
ASE-C
ACE-C
Time (sec)
L
ASE-C
ACE-C
ΔF/F
Time (sec)
M
*
ΔF/F AUC
ASE-C
ACE-C

# Figure 2

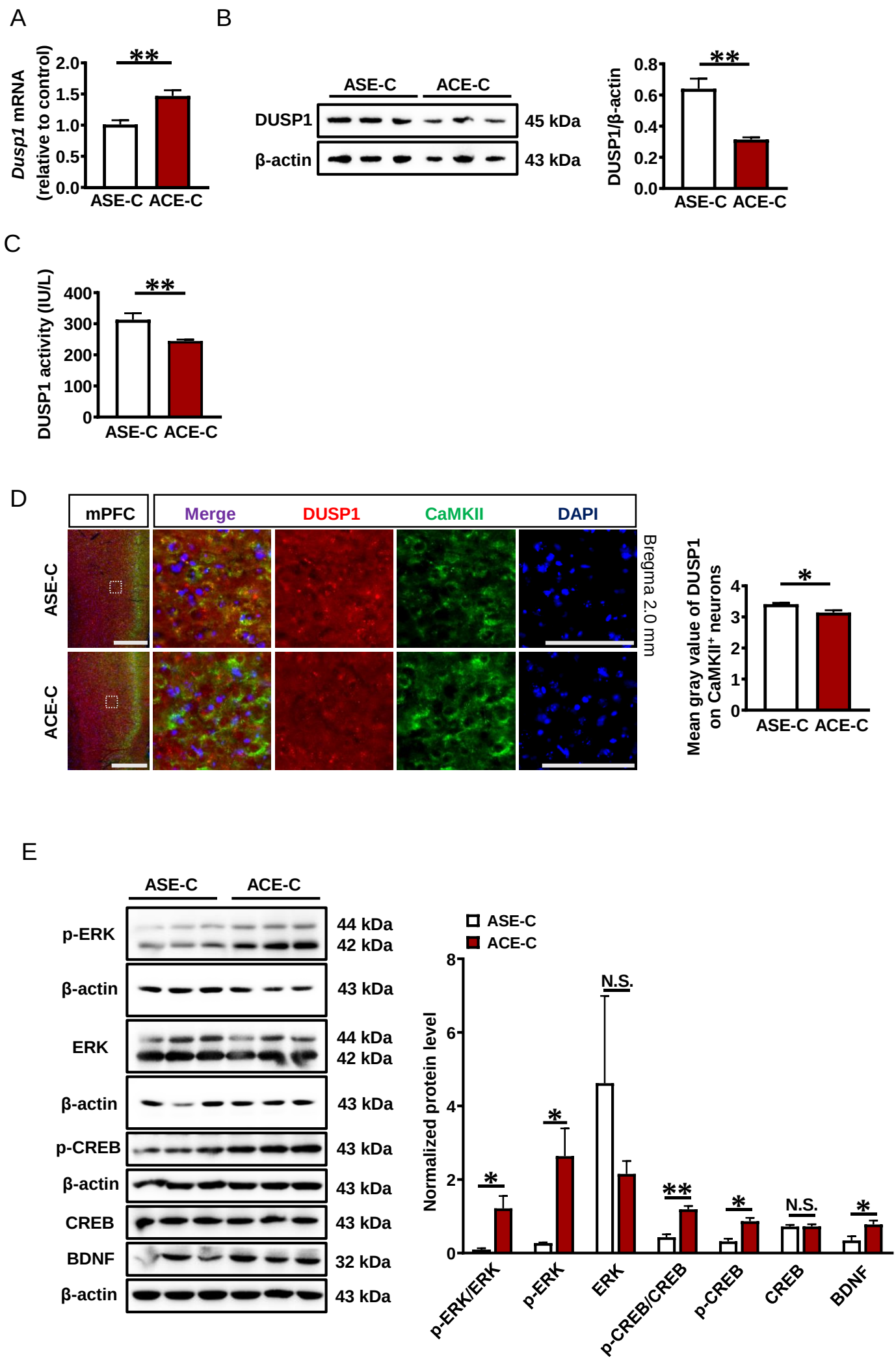
A
Dusp1 mRNA (relative to control)
2.0
1.5
1.0
0.5
0.0
**
ASE-C ACE-C
B
ASE-C
ACE-C
DUSP1
β-actin
45 kDa
43 kDa
DUSP1/β-actin
0.8
0.6
0.4
0.2
0.0
**
ASE-C ACE-C
C
DUSP1 activity (IU/L)
400
300
200
100
0
**
ASE-C ACE-C
D
mPFC
Merge
DUSP1
CaMKII
DAPI
ASE-C
ACE-C
Bregma 2.0 mm
Mean gray value of DUSP1 on CaMKII+ neurons
4
3
2
1
0
*
ASE-C ACE-C
E
ASE-C
ACE-C
p-ERK
β-actin
ERK
p-CREB
CREB
BDNF
44 kDa
42 kDa
43 kDa
32 kDa
Normalized protein level
8
6
4
2
0
N.S.
p-ERK/ERK
p-ERK
ERK
p-CREB/CREB
p-CREB
CREB
BDNF

# Figure 3

A

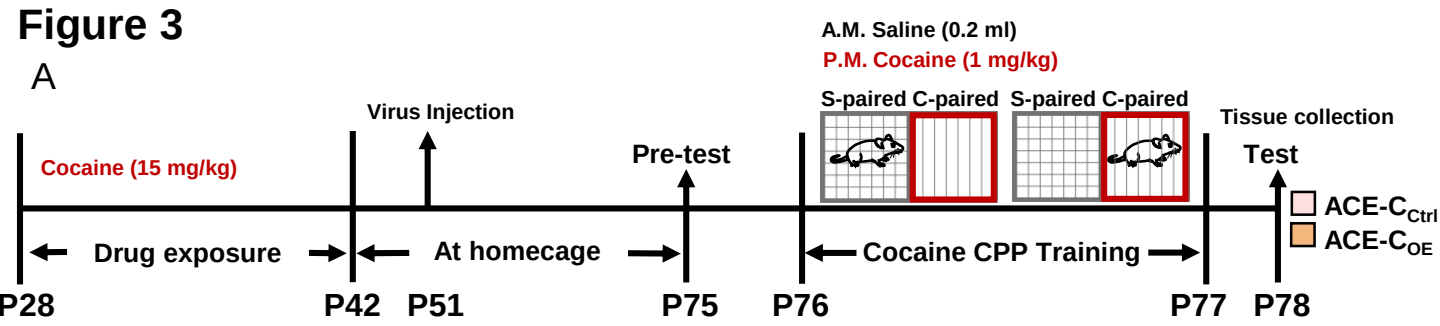


B

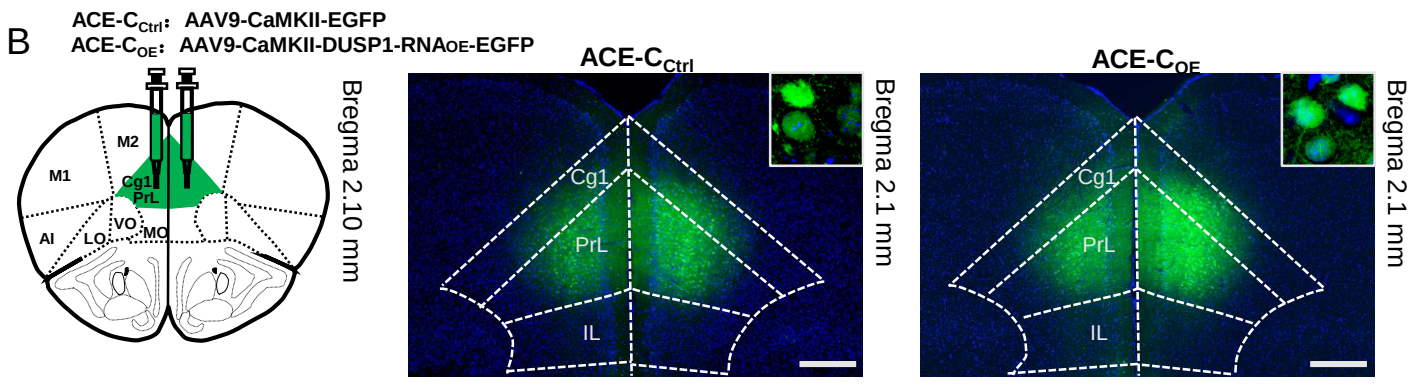


C

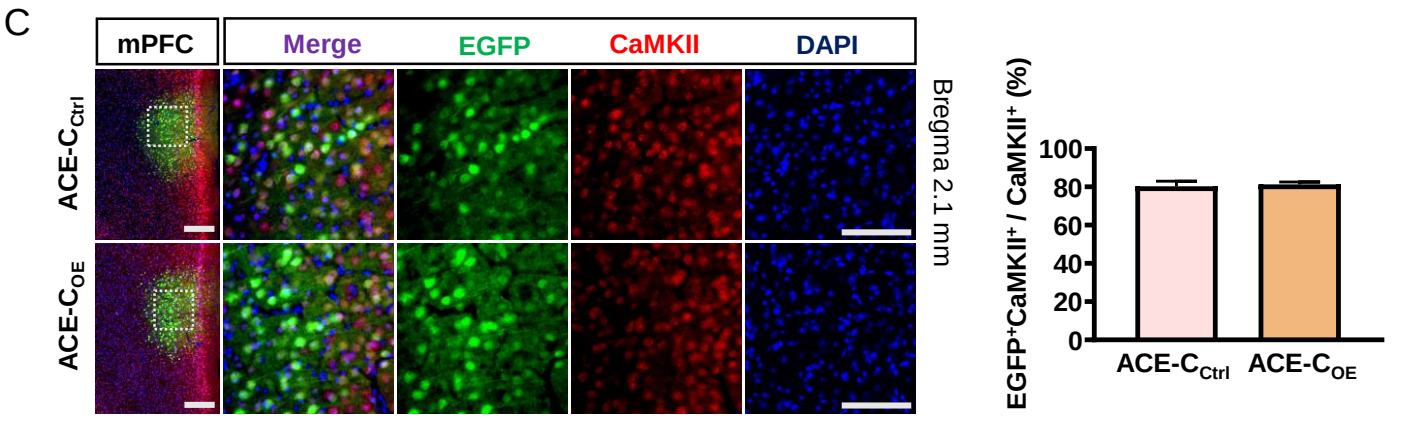


D

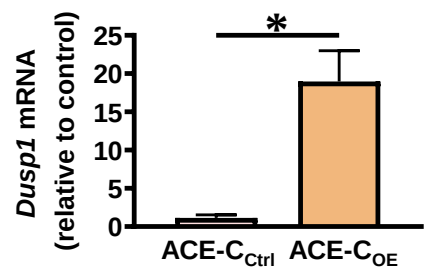


E

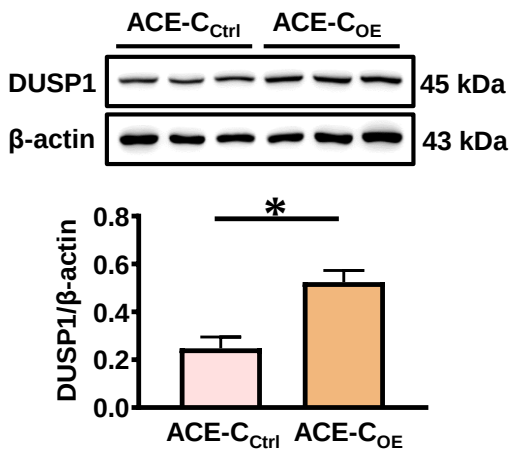


F

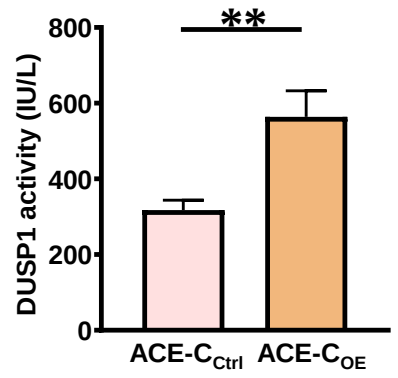


G

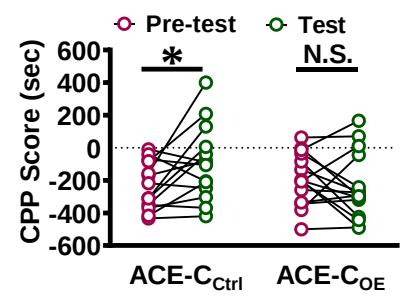


H

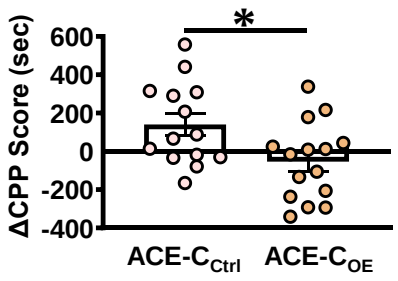


I

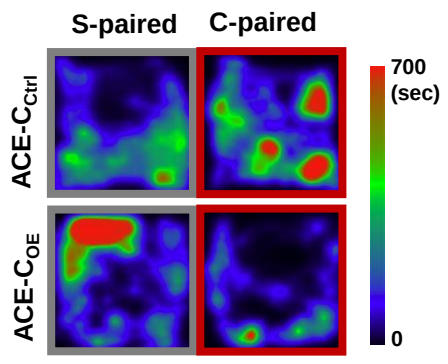


J

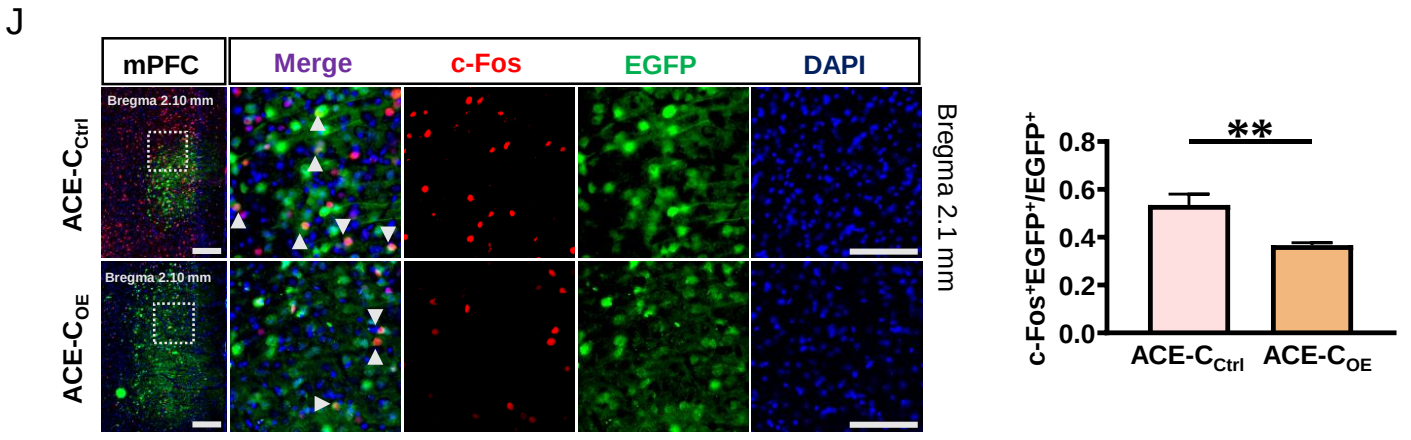


K

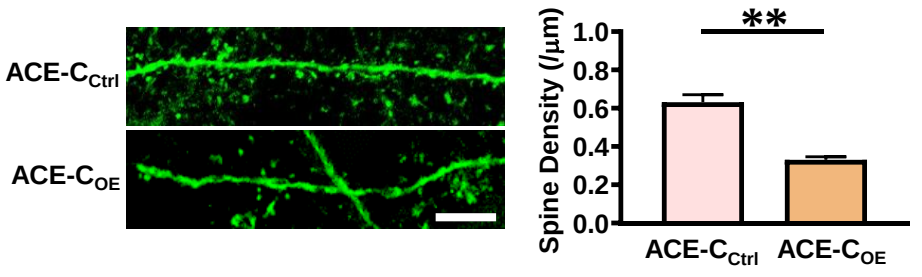


L

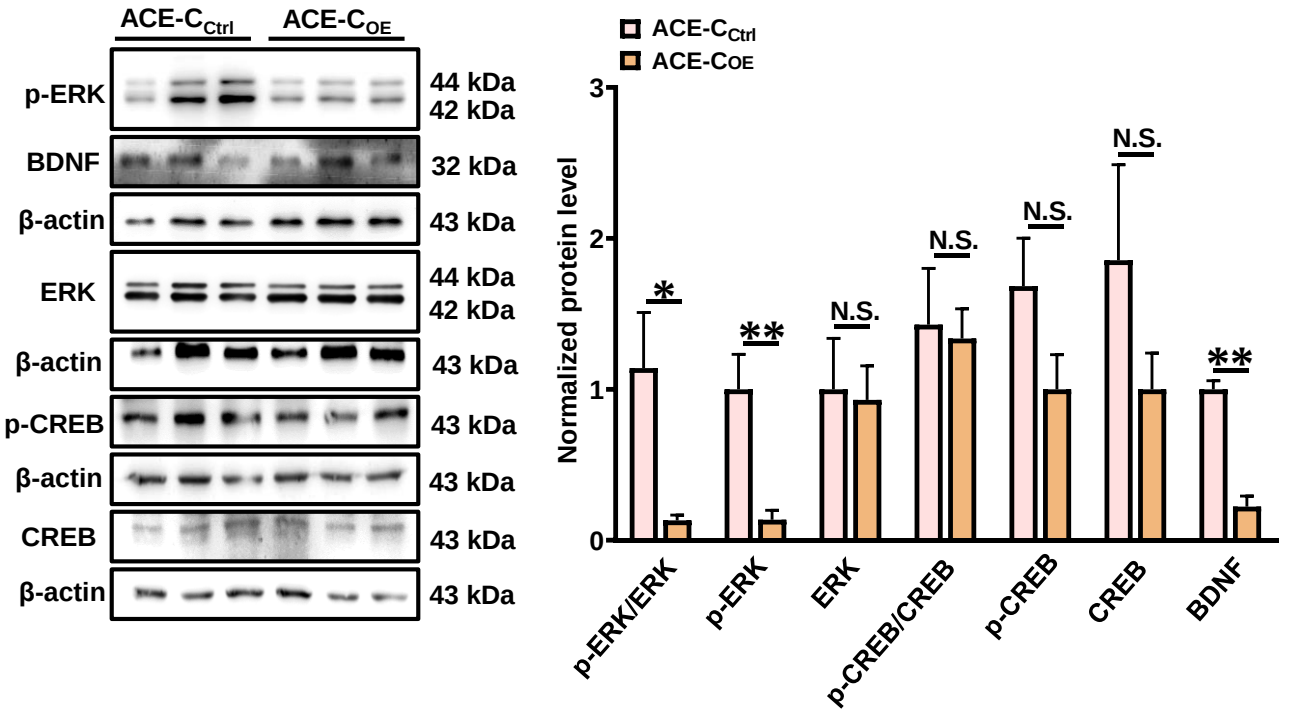

# Figure 4

A

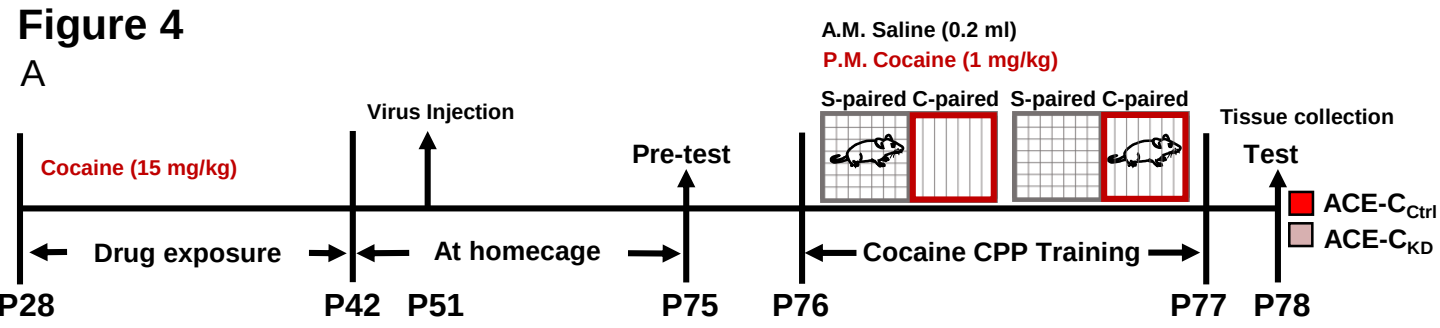


B

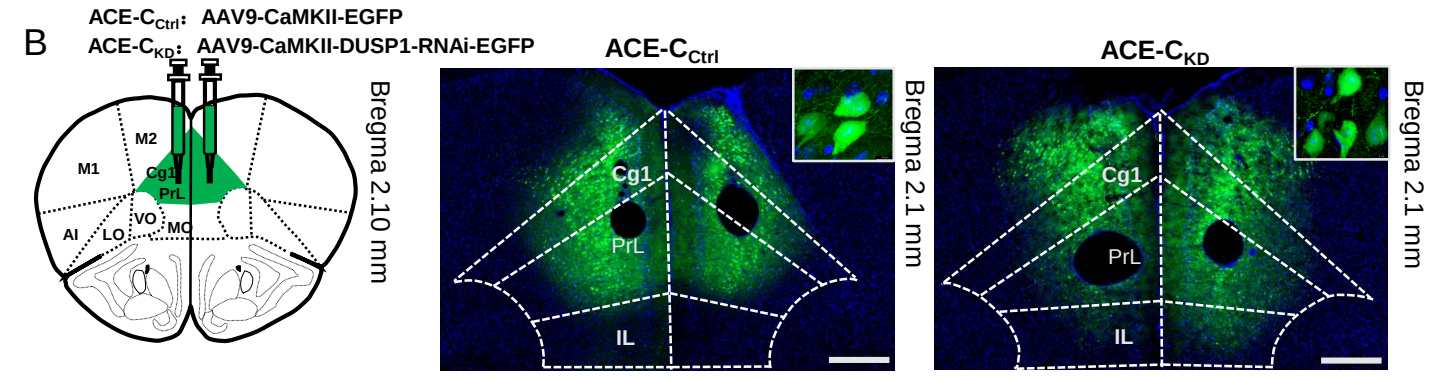


C

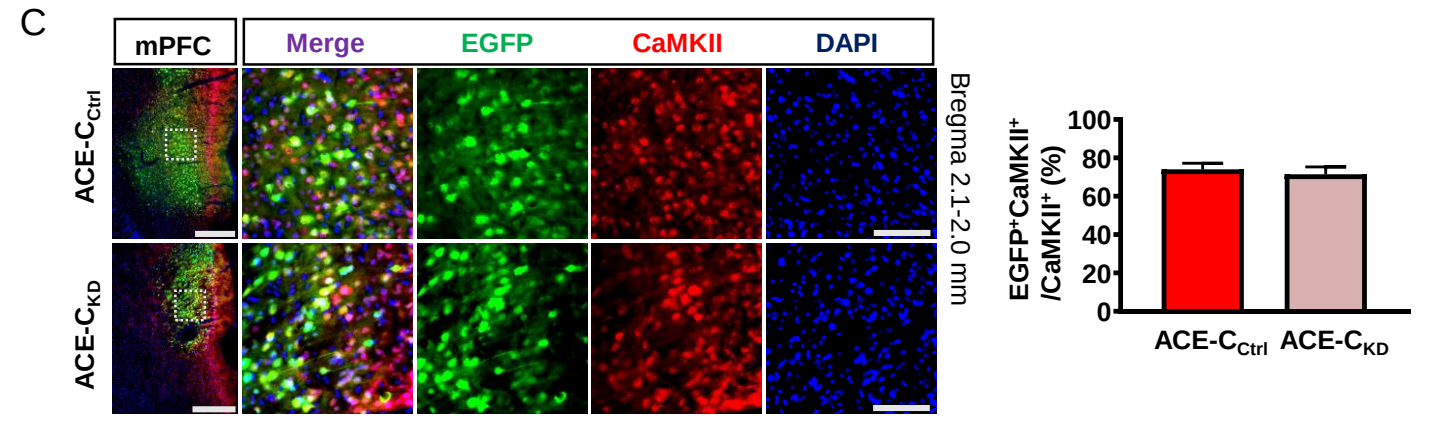


D

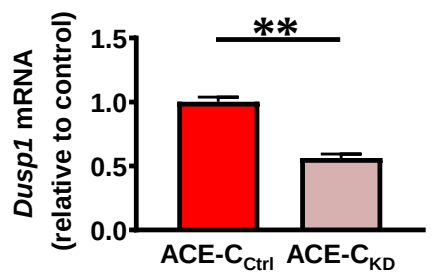


E

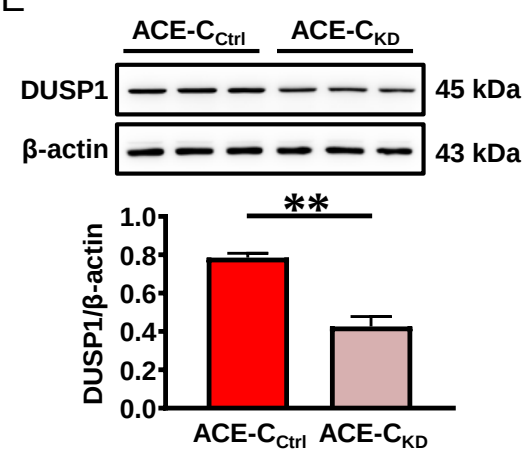


F

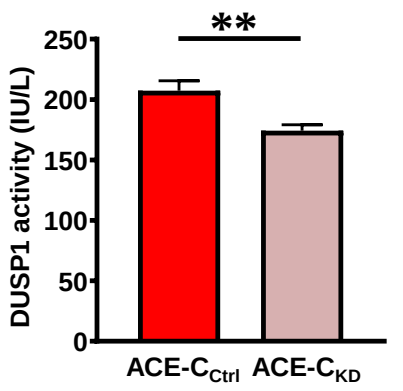


G

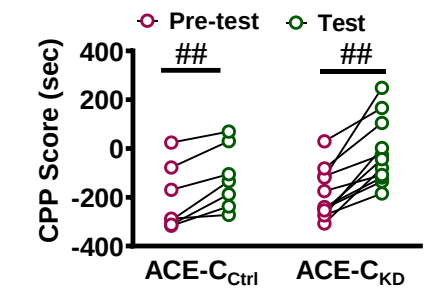


H

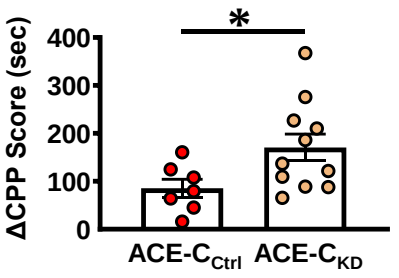


I

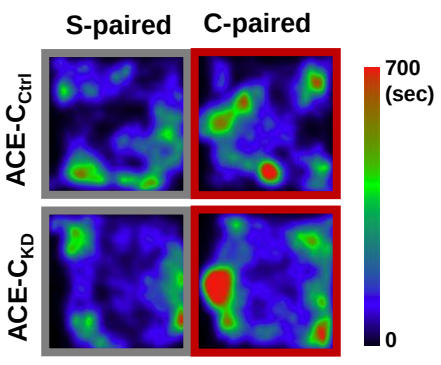


J

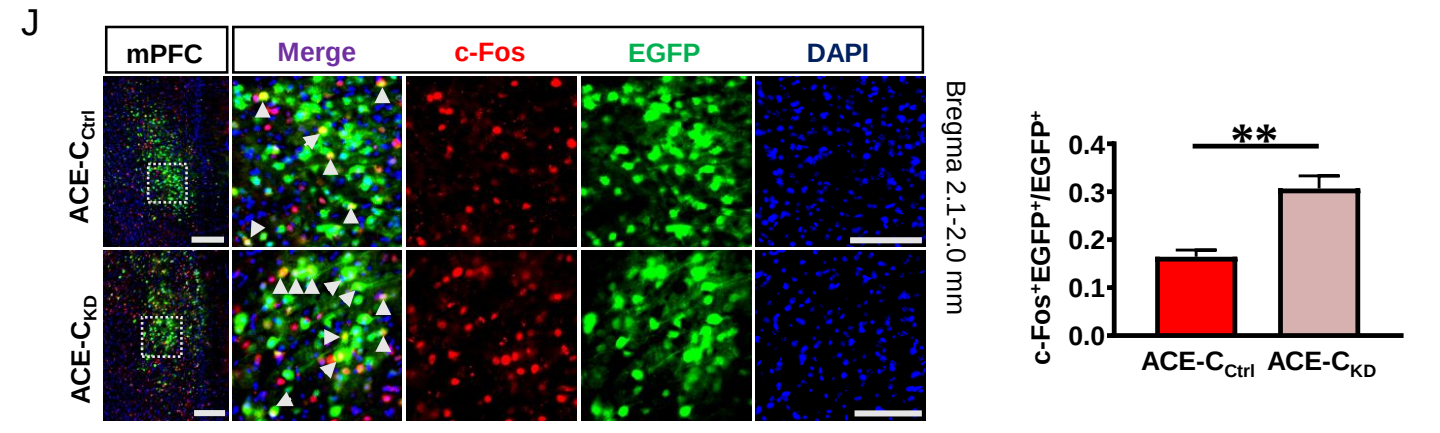


K

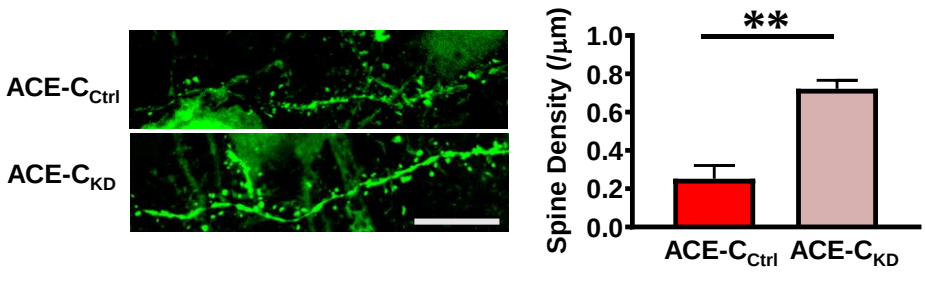


L

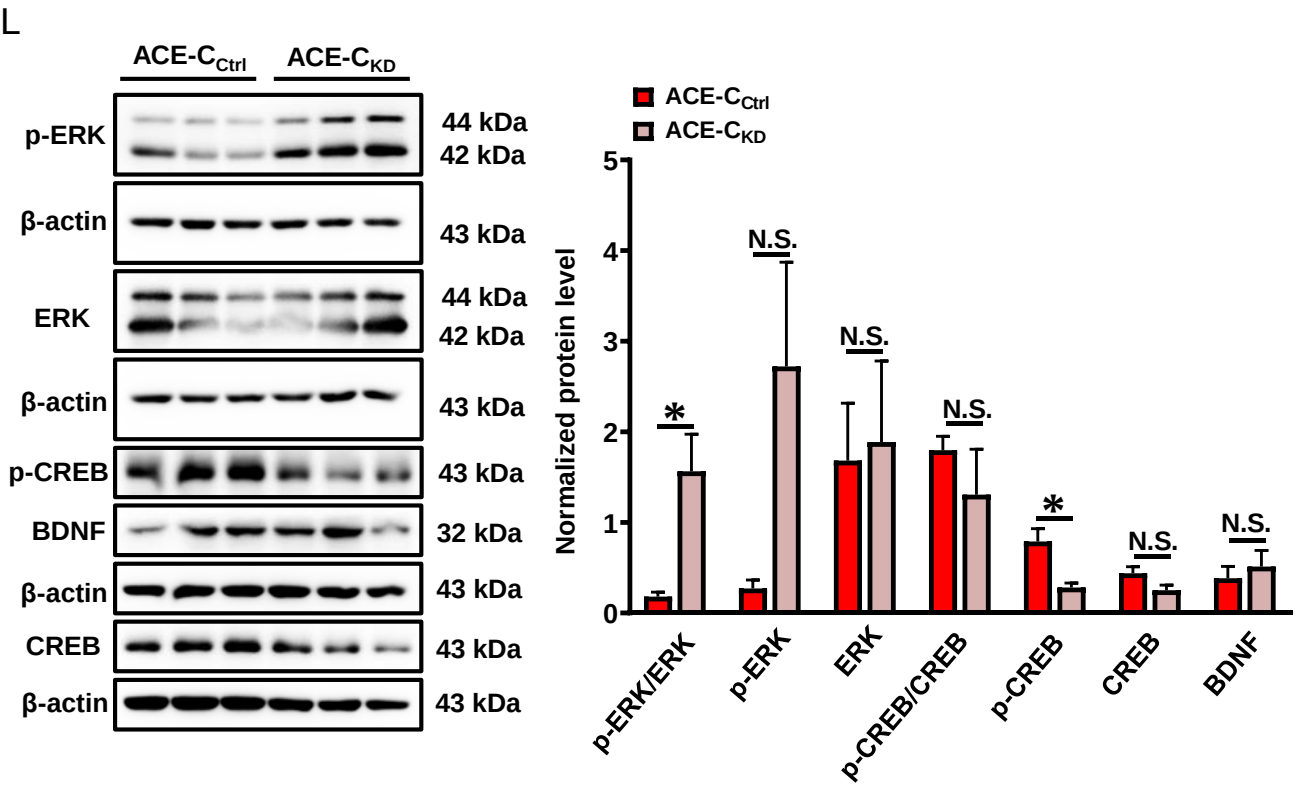

# Figure 5

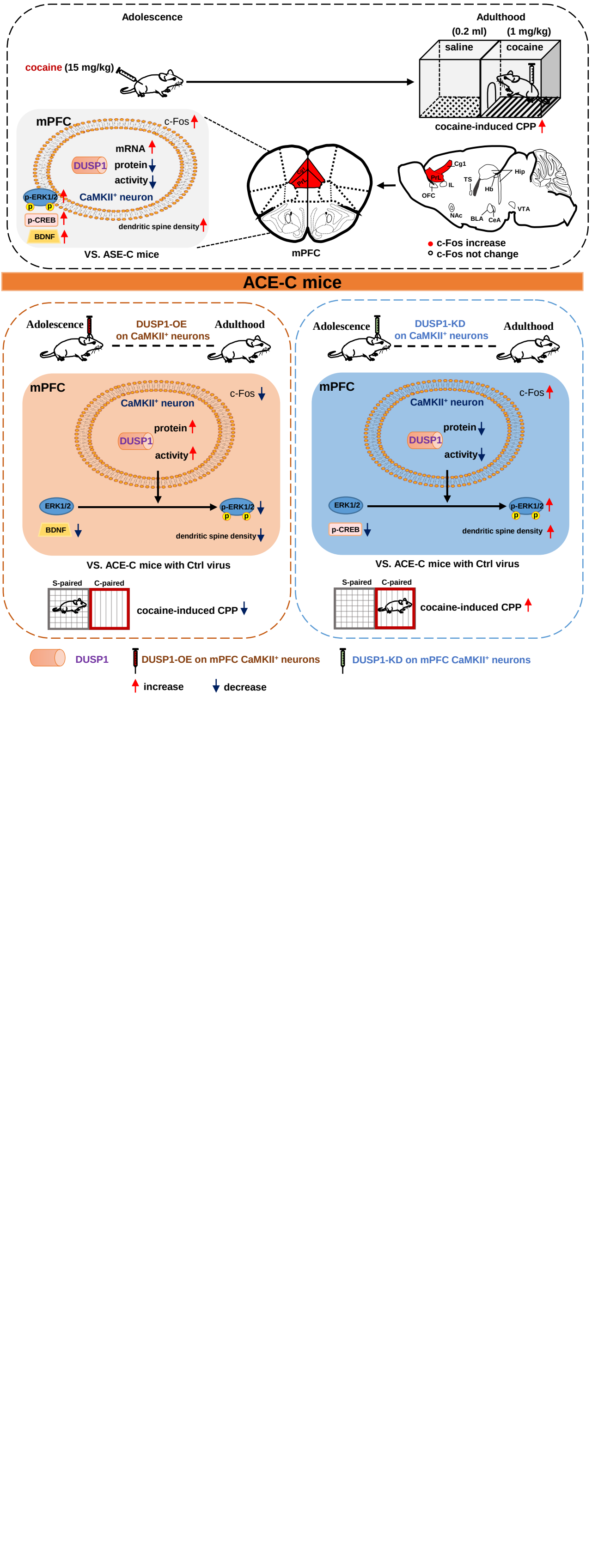
Adolescence
Adulthood
(0.2 ml)
(1 mg/kg)
saline
cocaine
cocaine (15 mg/kg)
cocaine-induced CPP
mPFC
c-Fos
mRNA
DUSP1
protein
activity
p-ERK1/2
CaMKII+ neuron
p-CREB
BDNF
dendritic spine density
VS. ASE-C mice
mPFC
Cg1
PrL
IL
OFC
TS
Hb
Hip
NAc
BLA
CeA
VTA
c-Fos increase
c-Fos not change
ACE-C mice
Adolescence
DUSP1-OE
on CaMKII+ neurons
Adulthood
mPFC
c-Fos
CaMKII+ neuron
protein
DUSP1
activity
ERK1/2
p-ERK1/2
BDNF
dendritic spine density
VS. ACE-C mice with Ctrl virus
S-paired
C-paired
cocaine-induced CPP
Adolescence
DUSP1-KD
on CaMKII+ neurons
Adulthood
mPFC
c-Fos
CaMKII+ neuron
protein
DUSP1
activity
ERK1/2
p-ERK1/2
p-CREB
dendritic spine density
VS. ACE-C mice with Ctrl virus
S-paired
C-paired
cocaine-induced CPP
DUSP1
DUSP1-OE on mPFC CaMKII+ neurons
DUSP1-KD on mPFC CaMKII+ neurons
increase
decrease

**Supplementary Data**

**Figure legends**

**Figure S1. The number of c-Fos-positive neurons in brain areas. A,** The number of c-Fos-positive neurons in brain areas of ASE-C and ACE-C mice. OFC, orbitofrontal cortex; Cg1, cingulate cortex; PrL, prelimbic cortex; IL, infralimbic cortex; NAc, nucleus accumbens; BNST, bed nucleus of the stria terminalis; TS, triangular septal nucleus; BLA, basolateral amygdala; CeA, central nucleus of the amygdala; mHb, medial habenula; LHb, lateral habenular; dCA1, vCA1, dorsal and ventral hippocampal CA1; dCA3, dorsal hippocampal CA3; dDG, dorsal dentate gyrus; VTA, ventral tegmental area. ASE-C, subthreshold-dosed administration of cocaine in adolescent saline-exposed mice; ACE-C, subthreshold-dosed administration of cocaine in adolescent cocaine-exposed mice; N.S., $p > 0.05$ vs ASE-C mice.

**Figure S2. The c-Fos levels and staining in sublayers of mPFC subregions. A,** The baseline (P74) and cocaine-responsive (P78) protein levels of c-Fos. **B,** The number of c-Fos-positive neurons in layer2/3 and layer5 of Cg1, PrL, IL. **C,** The correlation analysis of ΔCPP Score with c-Fos staining. The closer r to 1, the stronger the correlation between the two variables. $p < 0.05$, significantly correlated. **D,** The number of c-Fos-positive GAD67-labeled, PV-labeled or SOM-labeled neurons in mPFC. Cg1, cingulate cortex; PrL, prelimbic cortex; IL, infralimbic cortex. ASE-C, subthreshold-dosed administration of cocaine in adolescent saline-exposed mice; ACE-C, subthreshold-dosed administration of cocaine in adolescent cocaine-exposed mice; N.S., $p > 0.05$, *, $p < 0.05$, **, $p < 0.01$ vs ASE-C mice.

**Figure S3. The mPFC gene expression in adult mice. A,** Volcano plot illustration showed the upregulated, downregulated and unchanged genes in response to cocaine

administration in adult mice. Each dot represents one gene. Red, blue and gray dots represent the significantly up-regulated, down-regulated and not changed genes. **B,** The Protein-Protein Interaction (PPI) network of up-regulated genes. **C,** The heatmaps of up-regulated genes. The gene clusters, which are initially the sample type, are presented along the horizontal axis. The threshold was set as $p$-value < 0.05, single sample gene expression amount exceeds 100. Columns represent samples, and rows show the different genes. Color scale, red for higher abundance, while purple for lower abundance. **D,** Top 30 of enriched GO terms of upregulated genes by the categories of BP, CC and MF. **E,** Top 20 of enriched KEGG pathways of upregulated genes. ASE-C, subthreshold-dosed administration of cocaine in adolescent saline-exposed mice; ACE-C, subthreshold-dosed administration of cocaine in adolescent cocaine-exposed mice.

**Figure S4. The baseline of protein levels and activity of DUSP1 in mPFC. A,** DUSP1 protein levels on P74. **B,** DUSP1 activity on P74. ASE, adolescent saline-exposed mice; ACE, adolescent cocaine-exposed mice; N.S., $p > 0.05$ vs ASE mice.

# Figure S1

A

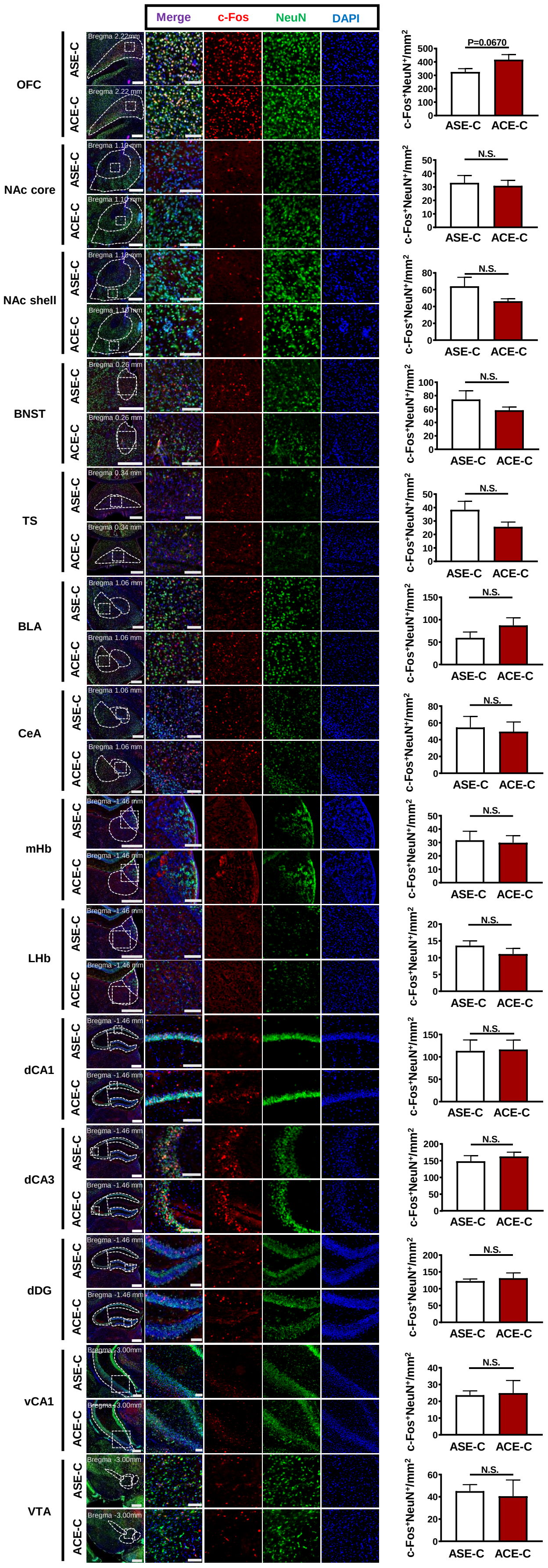
Merge
c-Fos
NeuN
DAPI
OFC
NAc core
NAc shell
BNST
TS
BLA
CeA
mHb
LHb
dCA1
dCA3
dDG
vCA1
VTA
ASE-C
ACE-C
Bregma 2.22 mm
Bregma 1.10 mm
Bregma 0.26 mm
Bregma 0.34 mm
Bregma 1.06 mm
Bregma -1.46 mm
Bregma -3.00mm
c-Fos+NeuN+/mm2
P=0.0670
N.S.
ASE-C
ACE-C

# Figure S2

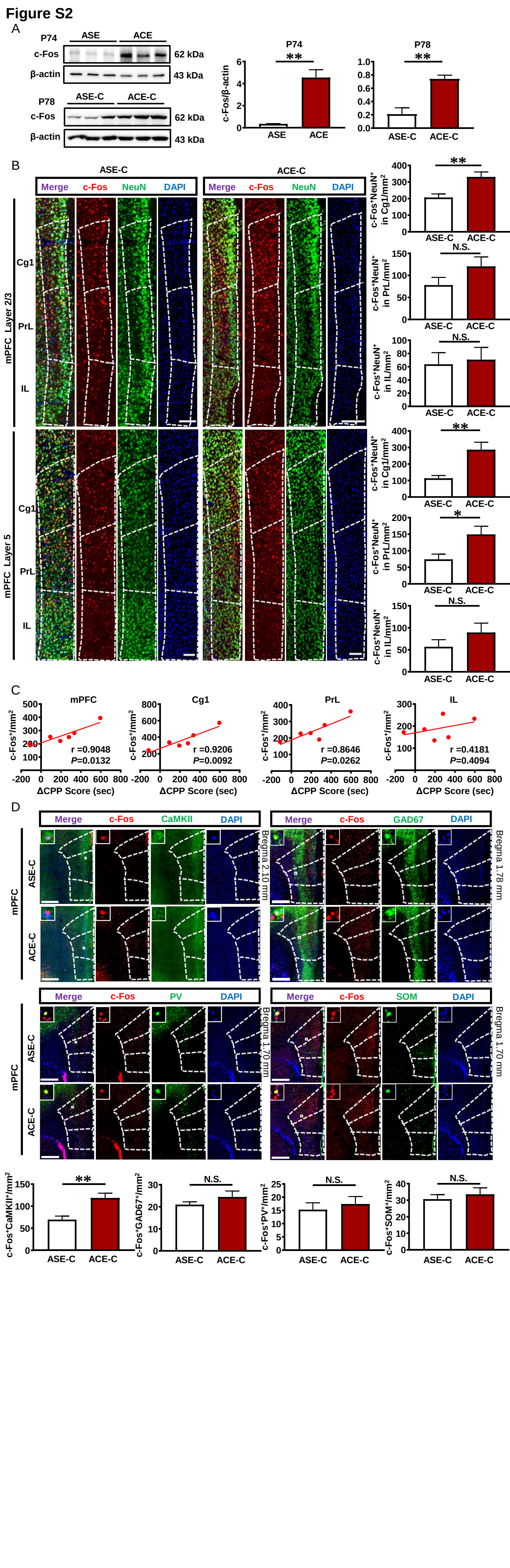
A
P74
ASE
ACE
c-Fos
β-actin
62 kDa
43 kDa
P78
ASE-C
ACE-C
c-Fos/β-actin
**
B
ASE-C
ACE-C
Merge
c-Fos
NeuN
DAPI
mPFC Layer 2/3
mPFC Layer 5
Cg1
PrL
IL
c-Fos+NeuN+ in Cg1/mm2
c-Fos+NeuN+ in PrL/mm2
c-Fos+NeuN+ in IL/mm2
N.S.
*
C
mPFC
Cg1
PrL
IL
c-Fos+/mm2
r =0.9048
P=0.0132
r =0.9206
P=0.0092
r =0.8646
P=0.0262
r =0.4181
P=0.4094
ΔCPP Score (sec)
D
CaMKII
GAD67
PV
SOM
Bregma 2.10 mm
Bregma 1.78 mm
Bregma 1.70 mm
c-Fos+CaMKII+/mm2
c-Fos+GAD67+/mm2
c-Fos+PV+/mm2
c-Fos+SOM+/mm2

# Figure S3

A

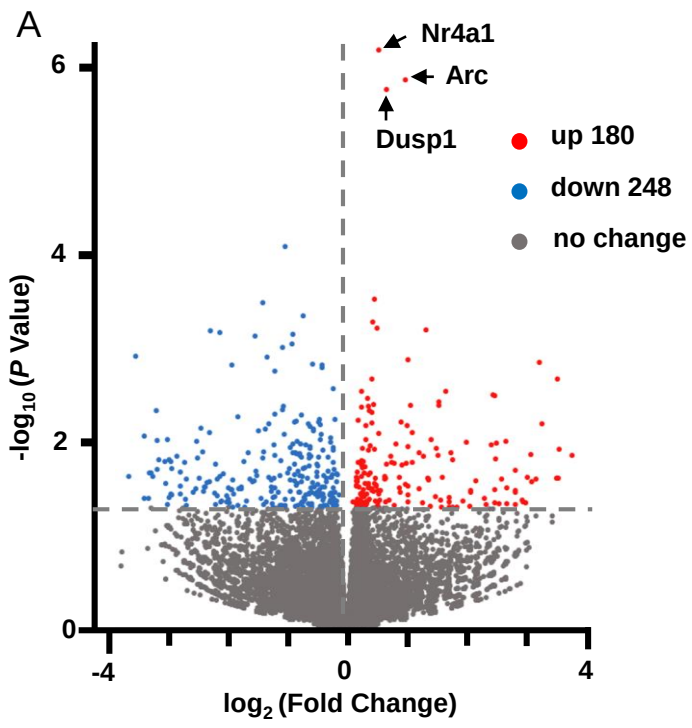


B

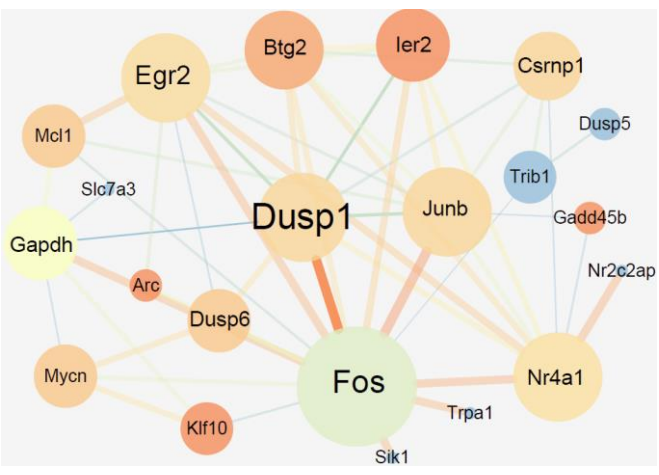


C

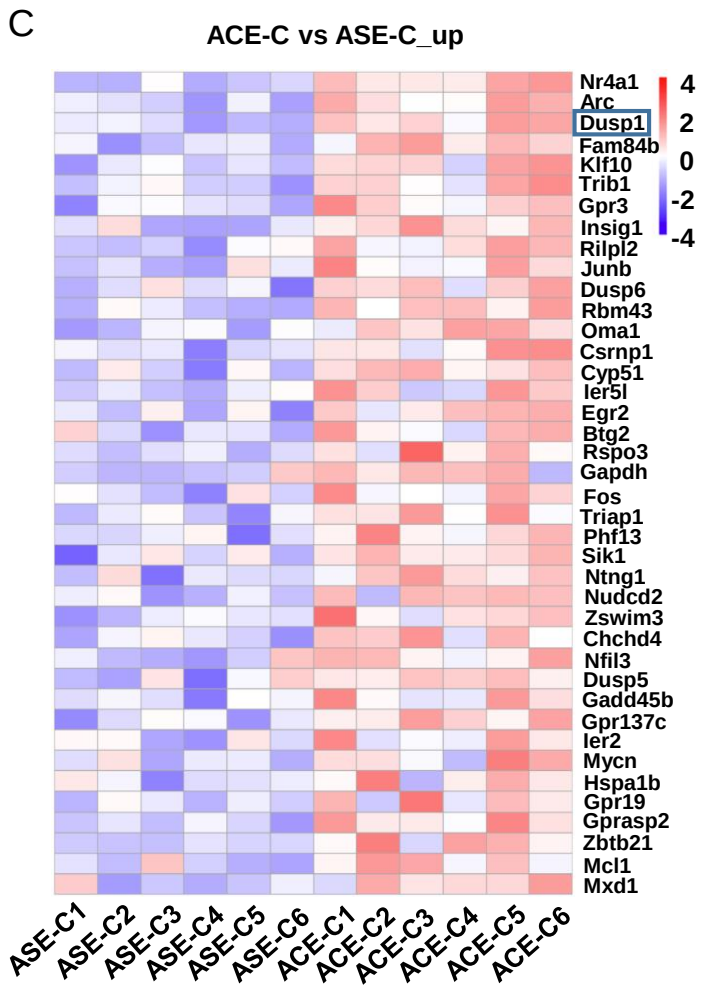


D

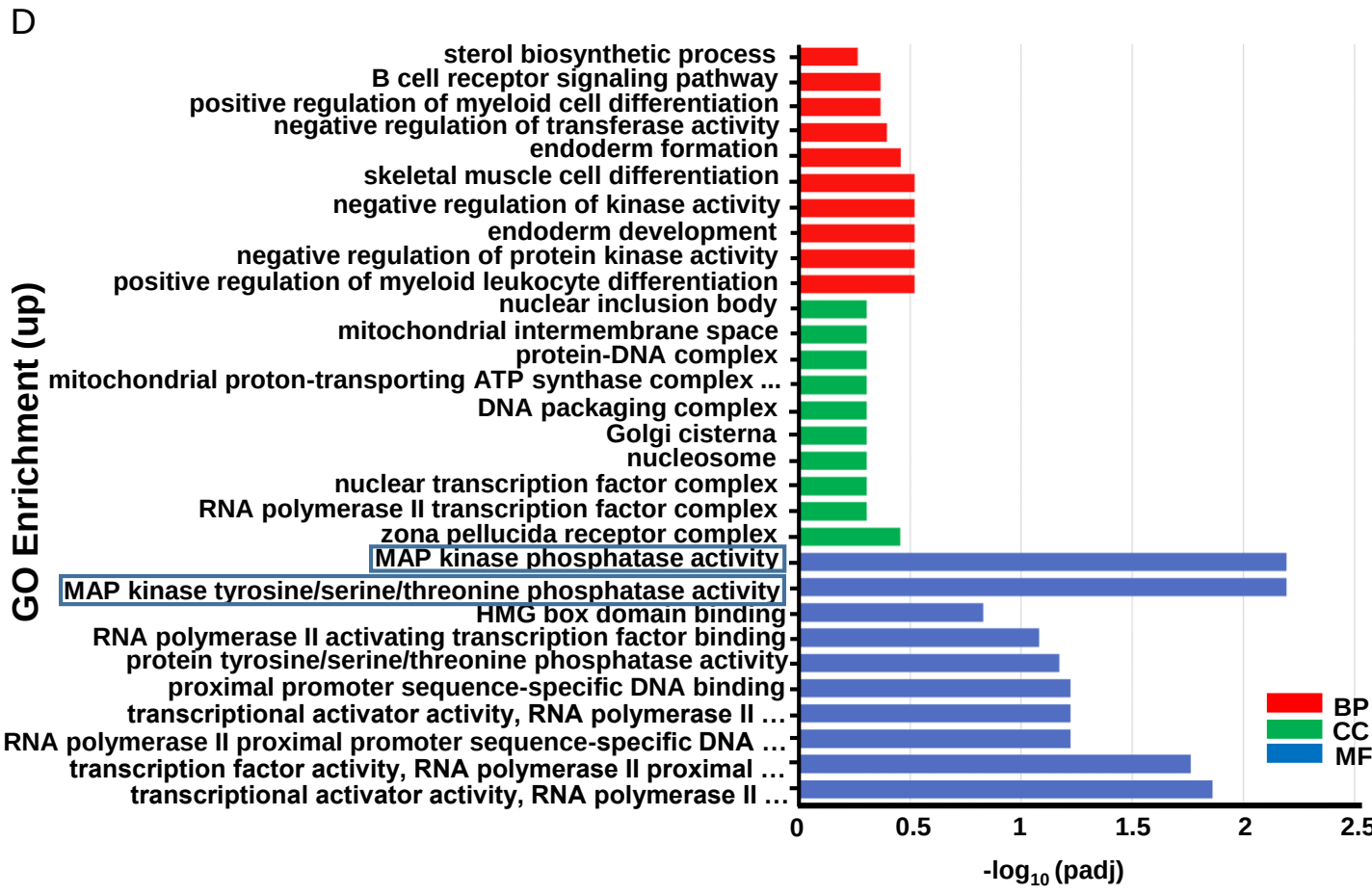


E

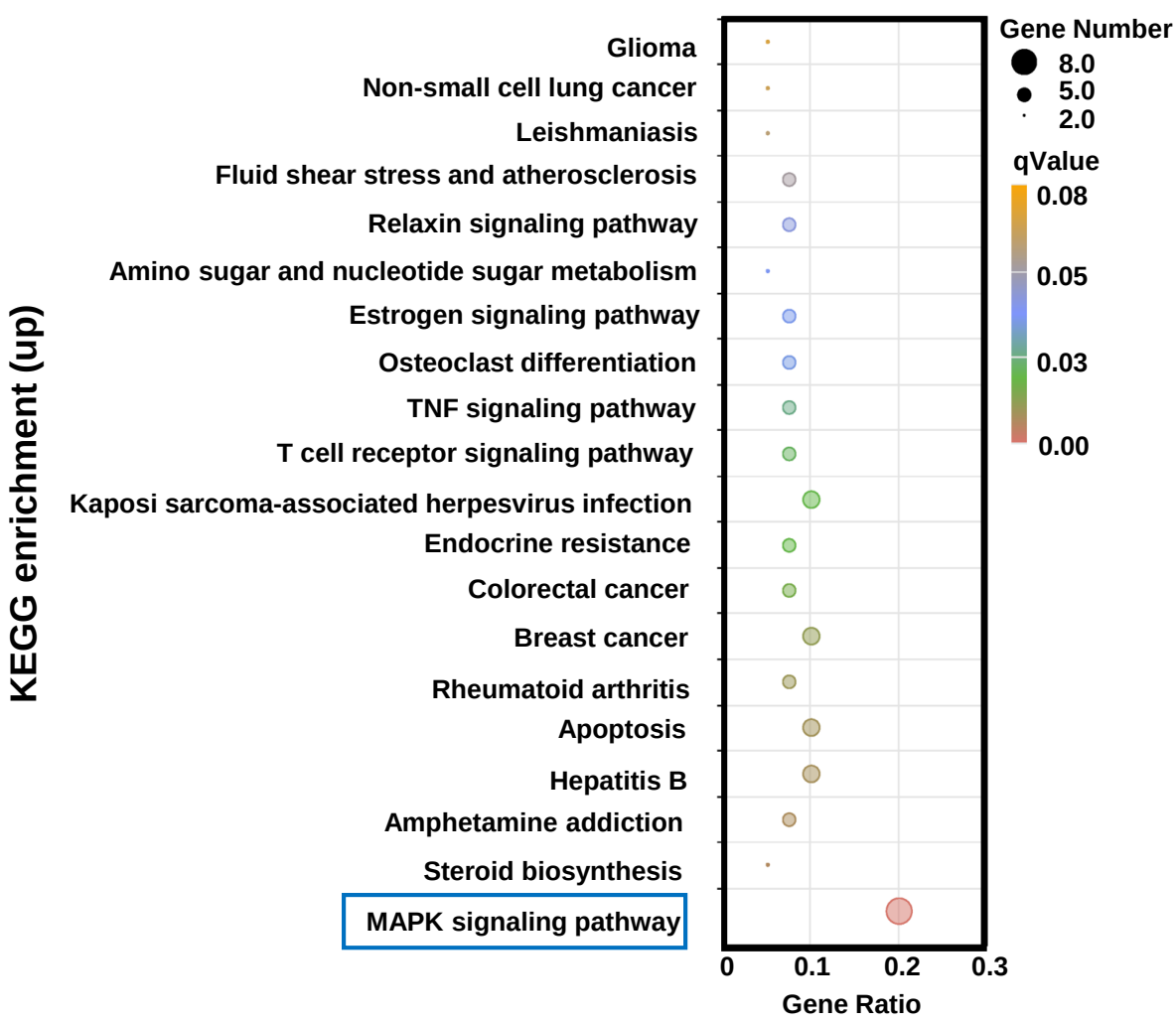

# Figure S4

A

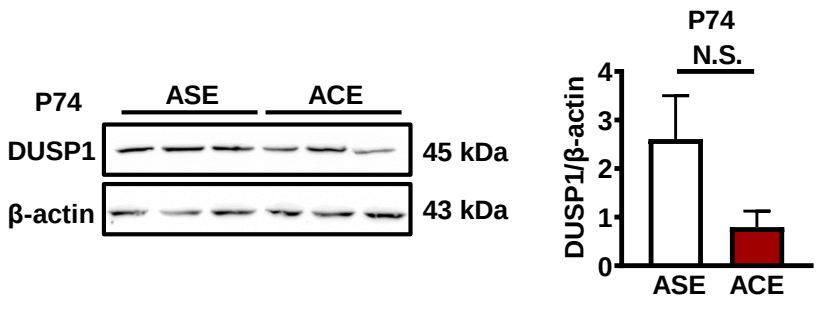
P74
ASE
ACE
DUSP1
45 kDa
β-actin
43 kDa
P74
N.S.
DUSP1/β-actin
4
3
2
1
0
ASE
ACE

B

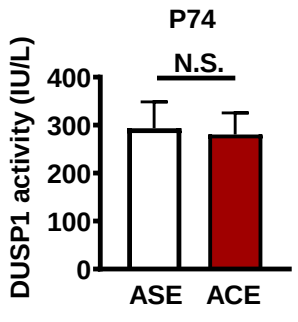
P74
N.S.
DUSP1 activity (IU/L)
400
300
200
100
0
ASE
ACE